from source patients who served as the source of the HCV infection, with the goal of elucidating the manner of HCV infection.

SUBJECTS AND METHODS

Patients

Between January, 1994 and December, 2000, 906 accidental exposures to blood-borne pathogens occurring within the facility of Osaka City University Hospital were reported to the Hepatitis Prevention and Research Center. At this hospital, each person exposed to blood-borne pathogens is followed for 1 year after the accident to check for the onset of hepatitis or hepatitis virus infection by hematological tests. The source patients for 448 of these accidents were HCV antibody-positive. Three people exposed to blood in three of these accidents developed acute hepatitis C. Using blood samples from these three recipient patients and two source patients, we evaluated the number of HCV clones and the degree of genetic diversity in HVR-1 of the HCV genome, using fluorescent single-strand conformation polymorphism and sequence analysis (FSSA; Otsuka Assay, Tokushima, Japan). It was not possible to collect blood from the source patient for R-Pt.2. Immediately after the accident, HCV antibody and HCV-RNA were both negative in the blood samples obtained from these three recipient patients. All three of these patients received interferon therapy. HCV antibody was measured by a second-generation enzyme-linked immunosorbent assay (Ortho Diagnostic Systems, Tokyo, Japan). HCV-RNA was quantified using Cobas Amplicore Monitor test (Version 2.0; Roche Diagnostic, Tokyo, Japan). Assays for HCV-RNA were performed at our facility [Nishiguchi et al., 1992].

Oligonucleotide Primers in the HVR-1

The primer sequences for the region were: HVR-1 (sense primer for first PCR): 5′-TGGGACACATGATGATGAACTGGT-3′: nt 1285–1308), HVR-2 (sense primer for second PCR: 5′-TACTACTCCATGGTGGGAGACTGGGC-3′: nt 1410–1435), HVR-3 (antisense primer for second PCR: 5′-GATGTGCCAGCTGCCATTGG-3′: nt 1576–1595), HVR-4 (antisense primer for first PCR and reverse transcription: 5′-CGGTGCTGTTTATGTGCCAACTGCC-3′: 1581–1605). These primers were obtained with an LKB Gene Assembler Plus DNA Synthesizer (Pharmacia Biotech, Uppsala, Sweden) using a protocol described previously [Schulhof et al., 1987]. The HVR-2 primer was labeled with fluorescein isothiocyanate (FITC), and the HVR-3 primer was labeled with biotin. The labeled second forward primer and the biotin-labeled second reverse primer for the FSSA method were synthesized.

HCV-RNA Extraction and Reverse Transcription

All serum samples were stored at −80°C. RNA was extracted from a 100 μl aliquot of serum sample as previously described [Chomczynski and Sacchi, 1987]. Reverse transcription from HCV-RNA to cDNA was performed using a protocol described previously [Sambrook et al., 1989].

Fluorescence Single-Strand Conformation Polymorphism (SSCP) Analysis

The number of quasispecies was determined by fluorescence SSCP analysis. PCR products were denatured for 5 min at 95°C in formamide dye (Pharmacia Biotech), and electrophoresed in 7% acrylamide gel (acrylamide: *N,N′*-methylenebisacryamide = 99:1) containing 5% glycerol and 7M urea using the ALF II DNA Sequencer (Pharmacia Biotech). The conditions of electrophoresis were as described in the technical manual supplied by the manufacturer. The electrophoresis buffer was tris-borate-ethylenediaminetetraacetic acid (TBE $2Na{\cdot}2H_2O$), and the fixed voltage was 1,500 V. The gel temperature was kept constant at 25°C with a water jacket. The upper limit of current was 45 mA, and the upper limit of power was 45 mW. The laser power was 3 mW and the time interval to collection of signal was once per 1.25 sec. Detection of HCV HVR-clone was carried out using the Fragment Manager (Amersham Pharmacia Biotech, Piscataway, NJ) software system.

Direct DNA Sequencing

PCR products were denatured by alkalizing, and then the biotin-labeled fragments were recovered with streptavidin-coated magnetic beads (Dynal, Oslo, Norway) using a protocol described previously [Hultman et al., 1989]. The sequencing reaction was performed using an auto read sequencing kit (Pharmacia Biotech) under the conditions recommended by the kit supplier, with a protocol based on the dideoxy-mediated chain-termination method.

RESULTS

Profiles of Recipient Patients at the Time of Diagnosis of Acute Hepatitis

In Case 1, the recipient patient 1 (R-Pt.1) was a male internist who accidentally punctured his finger with a needle after it was used for a drip infusion to a patient with chronic hepatitis C (source patient 1; S-Pt.1) on January 14, 1994. This recipient patient developed flu-like symptoms in March of the same year. On April 12, hematological tests revealed liver dysfunction. In Case 2, the recipient patient 2 (R-Pt.2) was a nurse, who accidentally cut her finger with a scalpel used for surgery on an HCV-positive patient on November 26, 1996. On December, 20 of the same year, this nurse was found to have liver dysfunction on hematological testing. In Case 3, the recipient patient 3 (R-Pt.3) was a female surgeon, who accidentally punctured her finger with a needle during surgery on an HCV-positive patient 3 (S-Pt.3) on June 19, 2000. On July 25 of the same year, this surgeon was found to have liver dysfunction on hematological examination. Immediately

after the accident, all three of these recipient patients were HCV antibody-negative. Table I shows the alanine aminotransferase (ALT), total bilirubin (T-bil), HCV-RNA level, HCV genotype, and HCV antibody titer results for these patients at the time of diagnosis of acute hepatitis. The mean length of time from accident to diagnosis was 49 days (range 24–88 days). Three recipient patients received IFN therapy. For R-Pt.1, natural IFN-alpha (Sumiferon, Sumitomo, Osaka, Japan) was administered for 15 consecutive days at 6 MIU/day, then for another 15 days at 9 MIU/day, and then three times a week for 6 weeks. However, the patient's ALT value remained abnormal. Therefore, IFN-alpha (9 MIU/day) was administered for another 15 consecutive days, then three times a week for 12 weeks (total dose: 855 MIU). For R-Pt.2, natural IFN-beta (Feron, Toray, Tokyo, Japan) was administered by injection for 38 consecutive days (6 MIU/day) beginning on day 59 after infection, and natural IFN-alpha (6 MIU/day) was administered for 14 consecutive days beginning on day 81 after infection, and three times a week during the subsequent 16-week period (total dose: 603 MIU). For R-Pt.3, natural IFN-alpha (Sumiferon, Sumitomo) was injected at a dose of 6 MIU for 14 consecutive days and three times a week during the subsequent 22-week period (total dose: 441 MIU). In all cases, HCV was successfully eradicated by IFN therapy.

Number of Quasispecies Measured by SSCP Analysis

Figure 1 shows the results of SSCP electrophoresis for each sample. The blood sampled from S-Pt.1 immediately after the accident contained 13 HCV clones. The blood sampled from R-Pt.1 on day 88 after the accident contained only two HCV clones. On day 101, the blood from this recipient patient contained four clones. Blood from R-Pt.2 contained two clones on day 24 and two clones on day 59 after the accident. In S-Pt.3, six clones were detected immediately after the accident. In R-Pt.3, four, two, and three clones were detected on day 39, 60, and 81 after the accident, respectively. Thus, the number of HCV quasispecies in blood from each recipient patient before the start of interferon therapy was smaller than that found in blood from the source patients examined immediately after the accident.

Analysis by Direct Sequencing

The genetic diversity of the HCV gene in blood from the source patients and recipient patients was analyzed by direct sequencing. In blood from S-Pt.1 collected immediately after the accident, genetic diversity was observed at 36 sites. On day 455, genetic diversity was observed at 34 sites. Thus, high genetic diversity continued to be observed in this patient. In R-Pt.1, who was exposed to blood from the source patient, variation was observed at two and four sites when examined on day 88 and 101 (at the start of IFN therapy) after the accident, respectively (Fig. 2). In S-Pt.3, base variations were observed at 20 sites immediately after the accident; however, no base variation of HCV was observed in blood sampled on day 39, 61, and 82 (start of IFN therapy), as shown in Figure 3. R-Pt.2 exhibited no variation on day 24 and 59 (not illustrated). Table II summarizes the number of HCV quasispecies and genetic diversity in individual patients. The number of quasispecies and genetic diversity for recipient patients during the period from the onset of hepatitis to the start of treatment were lower than those of source patients.

DISCUSSION

It is known that HCV quasispecies are found among HCVs of the same genotype detected in the same patient [Kato et al., 1993]. The presence of HVR-1 is known for the E2/NS1 region of the HCV envelope. The base sequence of HVR undergoes changes within individual HCV-infected patients [Ogata et al., 1991; Martell et al., 1992; Higashi et al., 1993]. It has been reported that variation in HVR base sequence becomes greater as the HCV-infected period becomes longer [Okamoto et al., 1992]. However, it was shown that the evolution rate of HCV domain strains was greater at the early stages of the infection than during the chronic phase [Cabtalobe et al., 2003]. In the present study, we measured HCV quasispecies, including HCV minor strains, and showed that the number of HCV quasispecies was smaller in recipients than in source patients. It is also known that HVR base sequences can be modified by treatment

TABLE I. Profiles of Recipient Patients at the Time of Diagnosis of Hepatitis

					At day of diagnosis of acute hepatitis C				
Case	Job	Sex	Age	Length of time to diagnosis (days)	Alanine aminotransferase (ALT) (IU)	Total bilirubin (T-bil) (mg/dl)	HCV-RNA level[a] (KIU/ml)	HCV genotype	HCV antibody (COI)
1	Dr	M	24	88	534	1.1	100	1b	4.7<
2	Ns	F	24	24	514	0.6	<0.5[b]	1b	4.7<
3	Dr	F	28	36	1,024	1.4	850	1b	(−)

Dr, doctor; Ns, nurse.
[a]Measured by the Cobas Amplicore Monitor test (version 2.0).
[b]HCV-RNA was positive by assays performed at our facility.

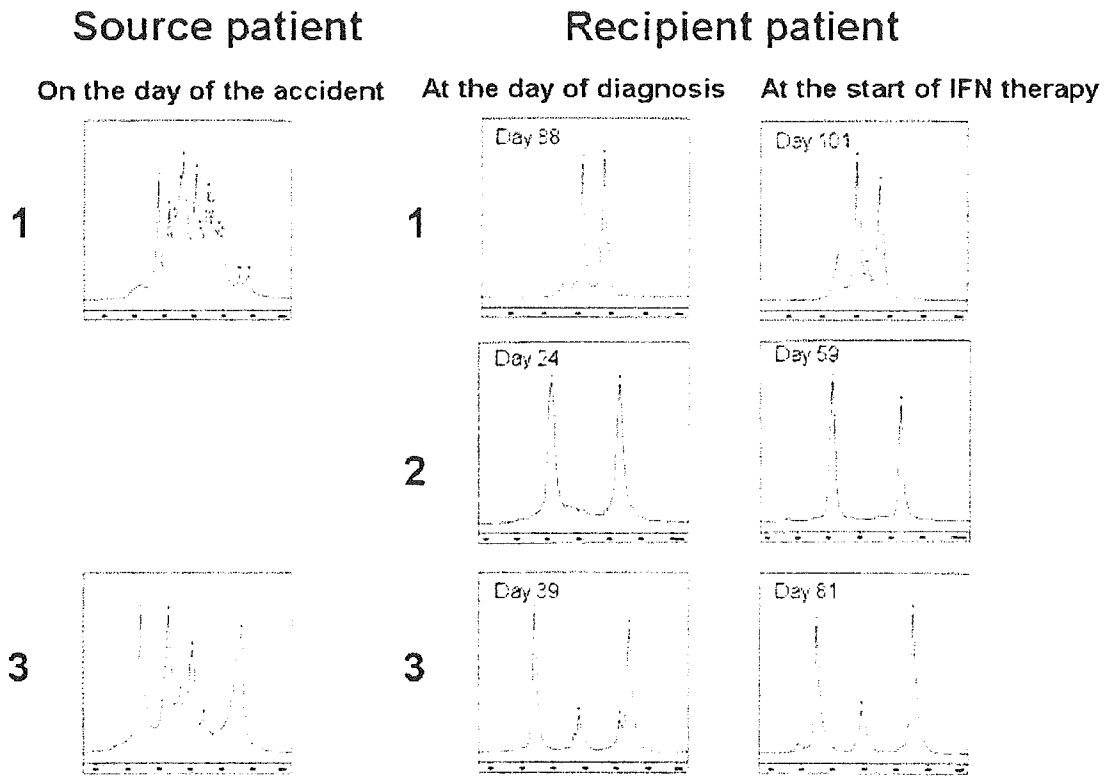

Fig. 1. Clone numbers determined by single-strand conformation polymorphism (SSCP) analysis of HCV hypervariable region-1 (HVR-1). Figures at left indicate the pattern of source patients immediately after the accident. Figures at center indicate the pattern of recipient patients at the time of diagnosis of acute hepatitis. Figures at right indicate the pattern of recipient patients at the start of IFN therapy.

Source patient 1

On the day of the accident

```
1         10         20         30         40         50         60         70
RCGACTWMSRYRWCGGGGGGGKYTRCTGSCHDYACCRYSYWWMGCMTCRYRRGMYTMYTCRCRHSTGGGCCGKCT
G-----AAGGTGA--------GT-G---G-AGT---GTGTAAA--A--GTGG-AT-AT--G-GAG-------G--
A-----TCCACAT--------TC-A---C-CAC---ACCCTTC--C--ACAA-CC-CC--A-ACC-------T--
------------------------------TT-------------------------------T-----------
```

455 days after the accident

```
1         10         20         30         40         50         60         70
RCGACYMMSRYRWCGGGGGGGKYTRCTGSCHRYACCRYSYWWMGCCTCRBRGGSMTCYTCRHVTBTGGGCSGTCT
G----TAAGGTGA--------GT-G---G-AGT---GTGTAAA-----GGG--GA--T--GAG-G-----G----
A----CCCCACAT--------TC-A---C-CAC---ACCCTTC-----ATA--CC--C--ACC-T-----C----
------------------------------T------------------C-----------TA-C----------
```

Recipient patient 1

88 days after the accident

```
1         10         20         30         40         50         60         70
ACGACTATGGTGTCGGGGGGGGGCTGCTGGCCATACCATGTTTAGCTTNANGGGCTTACTCACATCTGGGCCGTCT
-------------------------------------------------G-G-------------------------
-------------------------------------------------A-A-------------------------
-------------------------------------------------T-T-------------------------
-------------------------------------------------C-C-------------------------
```

At the start of IFN therapy (101 days after the accident)

```
1         10         20         30         40         50         60         70
ACGACTATGGTGTCGGGGGGGGGCTGCTGGCCATACCATGTYTAGCTTYNYGGGCTTACTCACATCTGGGCCGTCT
-----------------------------------------T------TGT-------------------------
-----------------------------------------C------CAC-------------------------
-------------------------------------------------T-------------------------
-------------------------------------------------C-------------------------
```

Fig. 2. Analysis by direct sequencing. Genetic diversities of HVR-1 for source patient 1 (S-Pt.1) and recipient patient 1 (R-Pt.1) are shown. The uppermost column shows the combinations of nucleic acids read by sequencing. The sites marked G (guanine), A (adenine), T (thymine), and C (cytosine) are clones corresponding to a single base. Combinations of base sequences corresponding to the other abbreviations are shown in the second through fifth columns. For example, N indicates the presence of clones in which the given site has the base G, A, T, or C.

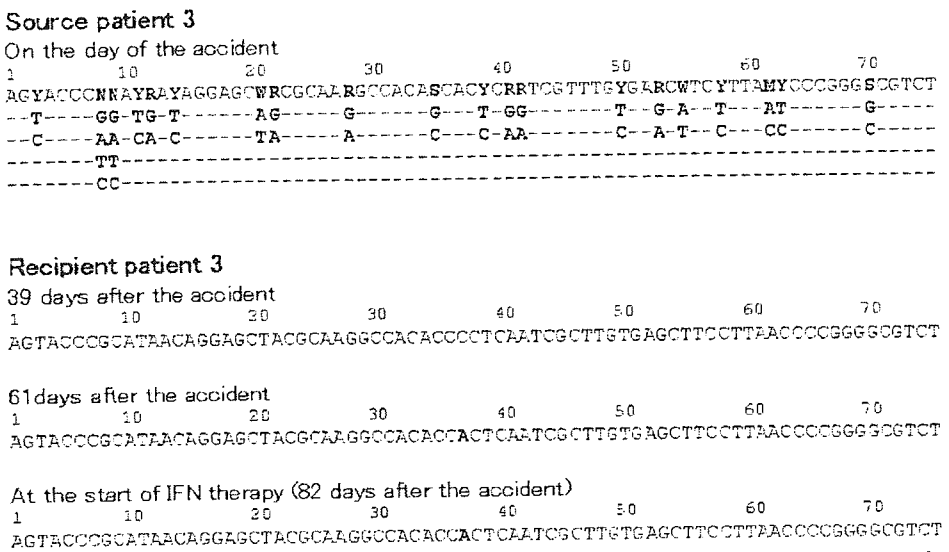

Fig. 3. Analysis by direct sequencing. Genetic diversities of HVR-1 for S-Pt.3 and R-Pt.3 are shown. The uppermost column shows the combinations of nucleic acids shown at sequencing. The sites marked G (guanine), A (adenine), T (thymine), and C (cytosine) are clones corresponding to a single base. Combinations of base sequences corresponding to the other abbreviations are shown in the second through fifth columns. For example, N indicates the presence of clones in which the given site has the base G, A, T, or C. In R-Pt.3, only one type of clone was revealed by sequencing at each of the three points of time.

with IFN or immunosuppressors [Okada et al., 1992; Higashi et al., 1993; Martell et al., 1994; Nishiguchi et al., 2002]. Changes in the amino acids constituting HVR can alter the three-dimensional structure of the virus [Taniguchi et al., 1993]. It has been suggested that HVR has B-cell epitopes, and their close relationship with escape from the host's immunosurveillance mechanisms has been pointed out. If variation in the HCV gene becomes large, response to IFN therapy may decrease [Farci et al., 1992; Weiner et al., 1992; Kato et al., 1993]. Toyoda et al. [1997] showed that when IFN was used for patients with chronic hepatitis C, the number of HCV quasispecies of HVR-1 was smaller in complete responders than in relapsing patients and non-responders, suggesting that this number can serve as the sole predictor of the likelihood of HCV-RNA disappearance during IFN therapy. Farci et al. [2000] calculated genetic distance between variants at the time of infection and at antibody seroconversion, and then showed that HCV genetic diversity was lower in patients who spontaneously eradicated HCV during the acute phase than in patients who became chronic carriers. Sequencing of multiple clones of HCV cDNA has shown that the composition of the HCV quasispecies changes. However, cloned cDNA may sometimes give a skewed picture of the mutant composition due to bias during the clone selection, and the technique makes it laborious to study more than a few patient samples. It has been

TABLE II. Time Course of Changes in Fluorescence Single-Strand Conformation Polymorphism and Sequence Analysis (FSSA) Results

	Source patient			Recipient patient		
Case	Days after the accident	Number of quasispecies	Genetic diversity	Days after the accident	Number of quasispecies	Genetic diversity
1	0	13	36			
				88	2	2
				101	4	4
	455	5	34			
2		ND	ND			
				24	2	0
				59	2	0
3	0	6	20			
				39	4	0
				60	2	0
				81	3	0

The results of FSSA analysis for source and recipient patients in Cases 1, 2, and 3 are shown chronologically. The day when the accident occurred was considered to be day 0. For each recipient patient, the uppermost column indicates the date of diagnosis of acute hepatitis and the lowest column shows the result for the serum sampled at the start of treatment.

demonstrated that HCV with the same number of SSCP bands at different times after liver transplantation has a different location and number of HVR-1 polymorphic sites [Yun et al., 1997]. The FSSA used in this study is not capable of directly measuring the base sequence of each clone, but can check for base variations of most clones. With this method, base variation can be detected if it is present in 6% of all strains, and clones can be detected if their amount is at least 1% of the HCVs in vivo (data from Otsuka Assay). When the number of base variations is smaller than the number of clones, clones account for only several percent of all strains. In the present study, we analyzed polymorphism of the HCV gene in blood from recipient patients who developed acute hepatitis C following accidental exposure to blood-borne pathogens at our hospital, and in serum samples collected from source patients immediately after the accident. As a result, it was confirmed that the number of HCV quasispecies was smaller, and that genetic diversity in blood from recipient patients was lower, than in blood sampled from source patients immediately after the accident. Kojima et al. [1994] demonstrated in experimental infection of chimpanzees that a population of HCV not bound to immunoglobulins was transmitted as a single population. In view of this finding, it seems likely that the HCV, which proliferates within the recipient patient following its transfer from the source patient via blood exposure, is not equivalent to the HCV found in the source patient.

In the acute stage of hepatitis C, the low genetic diversity and small number of quasispecies of the HCV proliferating within the recipient patient make it more probable that HCV will be eradicated by IFN therapy. Multiple clones, which differ little from each other in terms of base variation sites, differ little in terms of amino acids and have similar three-dimensional structures. These clones are likely to be eradicated together [Taniguchi et al., 1993].

In conclusion, when HCV infection has occurred from source patients with HCV in recipient patients due to exposure to blood, only a portion of the clones present in the blood of source patients can proliferate within recipient patients. These results suggest that starting IFN therapy for patients with acute hepatitis C during the stage of low HCV polymorphism will lead to greater success in eradication of HCV.

ACKNOWLEDGMENTS

The authors thank Megumi Kimura and Seiko Harima for technical assistance.

REFERENCES

Alter MJ, Margolis HS, Krawczynski K, Judson FN, Mares A, Alexsander WJ, Hu PY, Gerber MA, Sampliner RE. 1992. The natural history of community-acquired hepatitis C in the United States. The Sentinel Countries Chronic non-A, non-B Hepatitis Study Team. N Engl J Med 327:1899–1905.

Cabtalobe JF, Biangini P, Attoui H, Gallian P, MIco P, Lamballerie X. 2003. Evolution of hepatitis C virus in blood donors and their respective recipients. J Gen Virol 84:441–446.

Chomczynski P, Sacchi N. 1987. Single step method of RNA isolation by acid guanidinium thiocyanate-phenol-chloroform extraction. Anal Biochem 162:156–159.

Farci P, Alter HJ, Govindarajan S, Wong CD, Engle R, Lesniewski RR, Mushahwar KI, Desai MS, Miller HR, Ogata N, Purcell HR. 1992. Lack of protective immunity against reinfection with hepatitis C virus. Science 258:135–140.

Farci P, Shimoda A, Coiana A, Diaz G, Peddis G, Melpolder JC, Strzzera A, Chien DY, Munoz SJ, Balestrieri A, Purcell RH, Alter HJ. 2000. The outcome of acute hepatitis C predicted by the evolution of the viral quasispecies. Science 288:339–344.

Higashi Y, Kakumu S, Yoshioka K, Wakita T, Mizokami M, Ohba K, Ito Y, Ishikawa T, Takayanagi M, Nagai Y. 1993. Dynamics of genome change in the E2/NS1 region of hepatitis C virus in vivo. Virology 197:659–668.

Hultman T, Stahl S, Hornes E, Uhlen M. 1989. Direct solid phase sequencing of genomic and plasmid DNA using magnetic beads as solid support. Nucleic Acids Res 17:4937–4946.

Japanese Red Cross NAT Screening Research Group. 2000. Nationwide Nucleic acid amplification testing of hepatitis B virus, hepatitis C virus and human immunodeficiency virus and human immunodeficiency virus type 1 for blood transfusion and follow-up study of nucleic acid amplification positive donors. Jpn J Infect Dis 53:116–123.

Kato N, Sekiya H, Ootsuyama Y, Nakazawa T, Hijikata M, Ohkoshi S, Shimotohno K. 1993. Human immune response to hypervariable region 1 of the putative envelope glycoprotein (gp70) of hepatitis C virus. J Virol 67:3923–3930.

Kojima M, Osuga T, Tsuda F, Tanaka T, Okamoto H. 1994. Influence of antibodies to the hypervariable region of E2/NS1 glycoprotein on the selective replication of hepatitis C virus in chimpanzees. Virology 204:665–672.

Liddle C. 1996. Hepatitis C. Anaesth Intensive Care 24:180–183.

Martell M, Esteban JI, Quer J, Genesca J, Weiner A, Esteban R, Guardia J, Gomez J. 1992. Hepatitis C virus (HCV) circulates as a population of different but closely related genomes: Quasispecies nature of HCV genome distribution. J Virol 66:3225–3229.

Martell M, Esteban JI, Quer J, Vargas V, Esteban R, Guardia J, Gomez J. 1994. Dynamic behavior of hepatitis C virus quasispecies in patients undergoing orthotopic liver transplantation. J Virol 68:3425–3436.

Nakano Y, Kiyosawa K, Sodeyama T, Tanaka E, Matsumoto A, Ichijo T, Mizokami M, Furuta S. 1995. Acute hepatitis C transmitted by needlestick accident despite short duration interferon treatment. J Gastroenterol Hepatol 10:609–611.

Nishiguchi S, Kuroki T, Ueda T, Fukuda K, Takeda T, Nakajima S, Shiomi S, Kobayashi K, Otani S, Hayashi N, Shikata T. 1992. Detection of hepatitis C virus antibody in absence of viral RNA in patients with autoimmune hepatitis. Ann Intern Med 116: 21–25.

Nishiguchi S, Tanaka M, Shiomi S, Kaneshiro S, Enomoto M, Fukuda K, Tamori A, Habu D, Takeda T, Tohdoh N, Otani S, Tatsumi N. 2002. Changes in hypervariable region 1 in patients with chronic hepatitis C of genotype 1b with biochemical response to interferon. Hepatol Res 23:237–250.

Ogata N, Alter HJ, Miller RH, Purcell RH. 1991. Nucleotide sequence and mutation rate of the H strain of hepatitis C virus. Proc Natl Acad Sci USA 88:3392–3396.

Okada SI, Akahane Y, Suzuki H, Okamoto H, Mishiro S. 1992. The degree of variability in the amino terminal region of the E2/NS1 protein of hepatitis C virus correlates with responsiveness to interferon therapy in viremic patients. Hepatology 16:619–624.

Okamoto H, Kojima M, Okada S, Yoshizawa H, Iizuka H, Tanaka T, Muchmore EE, Peterson DA, Ito Y, Mishiro S. 1992. Genetic drift of hepatitis C virus during an 8.2-year infection in a chimpanzee: Variability and stability. Virology 190:894–899.

Omata M, Yokosuka O, Takano S, Kato N, Hosoda K, Imazeki F, Tada M, Ito Y, Ohto M. 1991. Resolution of acute hepatitis C after therapy with natural beta interferon. Lancet 338:914–915.

Sambrook J, Fritsch EF, Maniatis T. 1989. Molecular cloning. 2nd edn. Cold Spring Harbor, NY: Cold Spring Harbor Laboratory, 8.11p.

Schulhof JC, Molko D, Teoule R. 1987. The final deprotection step in oligonucleotide synthesis is reduced to a mild and rapid ammonia treatment by using labile base-protecting groups. Nucleic Acids Res 15:397–416.

Sodeyama T, Kiyosawa K, Urushihara A, Matsumoto A, Tanaka E, Furuta S, Akahane Y. 1993. Detection of hepatitis C virus markers and hepatitis C virus genomic-RNA after needlestick accidents. Arch Intern Med 153:1565–1572.

Taniguchi S, Okamoto H, Sakamoto M, Kojima M, Tsuda T, Tanaka E, Munekata E, Muchimore E, Peterson AD, Mishiro S. 1993. A structurally flexible and antigenically variable N-terminal domain of the hepatitis C virus E2/NS1 protein: Implication for an escape from antibody. Virology 195:297–301.

Toyoda H, Kumada T, Nakano S, Takeda I, Sugiyama K, Osada T, Kiriyama S, Sone Y, Kinoshita M, Hadama T. 1997. Quasispecies nature of hepatitis C virus and response to alpha interferon: Significance as a predictor of direct response to interferon. J Hepatol 26:6–13.

Weiner AJ, Geysen HM, Christopherson C, Hall JE, Mason TJ, Saracco G, Bonino F, Crawford K, Marion TJ, Crawford KA, Brunetto M, Barr PJ, Miyamura T, McHutchinson J, Houghton M. 1992. Evidence for immune selection of hepatitis C (HCV) putative envelope glycoprotein variant. Proc Natl Acad Sci USA 89:3468–3472.

Yun Z, Barkholt L, Sonnerborg A, 1997. Dynamic analysis of hepatitis C virus polymorphism in patients with orthotopic liver transplantation. Transplantation 64:170–172.

Int. J. Cancer: **118**, 1869–1876 (2006)
© 2005 Wiley-Liss, Inc.

Essential contribution of a chemokine, CCL3, and its receptor, CCR1, to hepatocellular carcinoma progression

Xiaoqin Yang[1], Peirong Lu[1], Chifumi Fujii[1,2], Yasunari Nakamoto[3], Ji-Liang Gao[4], Shuichi Kaneko[3], Philip M. Murphy[4] and Naofumi Mukaida[1,2]*

[1]*Division of Molecular Bioregulation, Cancer Research Institute, Kanazawa University, Kanazawa, Japan*
[2]*Center for the Development of Molecular Target Drugs, Cancer Research Institute, Kanazawa University, Kanazawa, Japan*
[3]*Department of Gastroenterology, Graduate School of Medicine, Kanazawa University, Kanazawa, Japan*
[4]*Laboratory of Molecular Immunology, National Institute of Allergy and Infectious Diseases, National Institutes of Health, Bethesda, USA*

We previously observed that a chemokine, macrophage inflammatory protein-1 α/CCL3, and its receptor, CCR1, were aberrantly expressed in human hepatocellular carcinoma (HCC) tissues. Here, we show that CCL3 and CCR1 are also expressed in 2 different models of this cancer; *N*-nitrosodiethylamine (DEN)-induced HCC and HCC induced by hepatitis B virus surface (HBs) antigen-primed splenocyte transfer to myelo-ablated syngeneic HBs antigen transgenic mice. At 10 months after DEN treatment, foci number and sizes were remarkably reduced in CCR1- and CCL3-deficient mice, compared with those of wild-type (WT) mice, although tumor incidence were marginally, but significantly, higher in CCR1- and CCL3-deficient mice than in WT mice. Of note is that tumor angiogenesis was also markedly diminished in CCL3- and CCR1-deficient mice, with a concomitant reduction in the number of intratumoral Kupffer cells, a rich source of growth factors and matrix metalloproteinases (MMPs). Among growth factors and MMPs that we examined, only MMP9 and MMP13 gene expression was augmented progressively in liver of WT mice after DEN treatment. Moreover, MMP9, but not MMP13, gene expression was attenuated in CCR1- and CCL3-deficient mice, compared with that of WT mice. Furthermore, MMP9 was expressed mainly by mononuclear cells but not hepatoma cells, and MMP9-expressing cell numbers were decreased in CCR1- or CCL3-deficient mice, compared with WT mice. These observations suggest the contribution of the CCR1-CCL3 axis to HCC progression.
© *2005 Wiley-Liss, Inc.*

Key words: angiogenesis; chemokine; carcinogenesis; Kupffer cell; matrix metalloproteinase

Chemokines are a large family of chemoattractant cytokines for leukocytes,[1,2] and their receptors belong to a family of specific G protein-coupled 7-transmembrane domain receptors.[3] A wide variety of tumor cells can produce various chemokines either constitutively or in response to various stimuli.[4] Then, chemokines can recruit various types of leukocytes, including monocytes/macrophages, lymphocytes and dendritic cells, thereby, modulating host responses to tumors. Moreover, several chemokines can control angiogenesis, a process essential for tumor growth, either directly or as a consequence of leukocyte infiltration and/or the induction of growth factor production.[5] Furthermore, some chemokines can guide the growth and the motility of tumor cells,[6] thereby, affecting the processes of tumor progression.

Hepatocellular carcinoma (HCC) is endemic in Asia, Africa and southern Europe, and ranks as the eighth most common cause of death among total human cancers. Most cases of HCC arise from chronic infection with human hepatitis B virus (HBV) or human hepatitis C virus (HCV).[7] Although several lines of evidence suggest the potential involvement of the chemokine interleukin-8/CXCL8 in the development of HCC,[8–10] other chemokines and their receptors may also play a role. In this regard, among various chemokine receptors including CCR1, 2, 3, 4 and 5, CXCR1, 2, 3 and 4, we observed previously that CCR1 was the only one expressed constitutively in all the 6 human hepatoma cell lines that we examined.[11] Moreover, CCR1 and its ligand CCL3 were also expressed abundantly by tumor cells and to a lesser degree, endothelial cells in human HCC tissue.[11] These observations suggest that the CCL3-CCR1 axis can exert its effects on tumor cells as well as endothelial cells in an autocrine or paracrine manner.

Chronic HBV or HCV infection can cause continuous and recurrent cycles of hepatocyte necrosis and regeneration, resulting in accumulation of mutations.[12] Etiological studies have demonstrated that cigarette smoking increases the risk of HCC significantly among patients with chronic HBV infection because it contains *N*-nitrosamines, a potent class of hepatocarcinogen.[13,14] Because *N*-nitrosodiethylamine (DEN), a specific *N*-nitrosamine, can cause HCC with a high frequency in rodents when administered to suckling animals,[15,16] the DEN-induced hepatocarcinogenesis model has been used to clarify the molecular mechanisms of hepatocarcinogenesis even though most cases of HCC arise from chronic infection of HBV or HCV.

Hence, to test the roles of CCL3 and CCR1 in hepatocarcinogenesis, we treated both WT mice and mice deficient in either *CCL3* or *CCR1* gene with DEN. Here, we provided the first definitive evidence on the contribution of the CCL3-CCR1 axis to HCC progression in an animal model.

Material and methods

Reagents

DEN was purchased from Sigma-Aldrich (St. Louis, MO). Rat anti-mouse F4/80 (clone: A3-1) and anti-CD34 (MEC 14.7) monoclonal antibodies were obtained from Serotec (Oxford, United Kingdom). Rabbit anti-mouse CCR1 antibodies were prepared[17] and kindly provided by Dr. Kouji Matsushima (University of Tokyo). Goat anti-mouse CCL3 and goat anti-mouse matrix metalloproteinase (MMP) 9 antibodies were obtained from R&D Systems (Minneapolis, MN).

Mice

Specific pathogen-free C57BL/6 mice were purchased from Charles River Japan (Yokohama, Japan) and designated as wild-type (WT) mice. CCL3-deficient mice[18] were obtained from Jackson Laboratories (Bar Harbor, ME) and CCR1-deficient mice were

Abbreviations: bFGF, basic fibroblast growth factor; DEN, *N*-nitrosodiethylamine; HBs, hepatitis B virus surface antigen; HBV, human hepatitis B virus; HCC, hepatocellular carcinoma; HCV, human hepatitis C virus; HGF, hepatocytes growth factor; IMVD, intratumoral microvessel density; MMP, matrix metalloproteinase; RT-PCR, reverse transcription-polymerase chain reaction; TIMP, tissue inhibitor of matrix metalloproteinase; VEGF, vascular endothelial growth factor; WT, wild-type.

Grant sponsor: Ministry of Education, Culture, Sports, Science and Technology of the Japanese Government.

*Correspondence to: Division of Molecular Bioregulation, Cancer Research Institute, Kanazawa University, 13-1 Takara-machi, Kanazawa 920-0934, Japan. Fax: 81-76-234-4520.
E-mail: naofumim@kenroku.kanazawa-u.ac.jp

Received 19 July 2005; Accepted after revision 1 September 2005
DOI 10.1002/ijc.21506
Published online 11 November 2005 in Wiley InterScience (www.interscience.wiley.com).

UICC

generated as described previously.[19] These deficient mice have been backcrossed to C57BL/6 mice for at least 8 generations and were kept under specific pathogen-free conditions. The preparation of HBsAg transgenic mice were described previously.[20] These mice contain the entire HBV envelope containing region (subtype ayw) under the constitutive transcriptional control of the mouse albumin promoter and express the HBV small, middle and large envelope proteins in their hepatocytes.[20] All animal experiments were performed in compliance with the Guideline for the Care and Use of Laboratory Animals on the Takara-machi Campus of Kanazawa University.

DEN-induced hepatocarcinogenesis model

Three-week-old weanling male mice were given a single intraperitoneal injection of DEN dissolved in physiologic saline solution at a dose of 10 μg/g of body weight.[21] Mice were killed 10 months after injection, for the evaluation of HCC development. When mice died before this time interval, the liver was removed to enumerate the number of tumors on the liver surface, larger than 1 mm, and to be fixed in 10% neutral-formalin buffer for histological analysis. In another series of experiments, mice were killed at the indicated time intervals after DEN treatment for histological analysis and extraction of total RNA.

Hepatocarcinogenesis model in HBs antigen transgenic mice

Hepatocarcinogenesis was induced in HBs antigen transgenic mice by replacing bone marrow cells and splenocytes derived from syngeneic non-transgenic mice immunized with HBs antigen, as previously described.[22] In this model, until 15 months after the splenocyte transfer, mice exhibited multiple HCC foci surrounded by non-tumor areas with hepatocytes, with an atypical nuclear configuration.

Histological analysis

Paraffin-embedded sections were cut at 5 μm and stained with hematoxylin and eosin solution. The numbers and sizes of the neoplastic foci were determined by an examiner without any prior knowledge about the experimental procedures, according to the method of Pierce,[23] with some modifications. The foci number per cm^2 and the percentage of the areas occupied with tumor foci were determined by using NIH Image analysis software ver 1.62 (National Institutes of Health, Bethesda, MD).

Immunohistochemical analysis

Rabbit anti-mouse CCR1 (5 μg/ml), goat anti-mouse CCL3 (10 μg/ml) or goat anti-mouse MMP9 antibodies (5 μg/ml) were used as the primary antibodies. The sections were further incubated with biotinylated goat anti-rabbit or rabbit anti-goat immunoglobulins as the secondary antibodies. The immune complexes were detected by using Vectastain Elite ABC kit and DAB Substrate Kit (Vector Laboratories, Burlingame, CA) according to the manufacturer's instructions. The slides were then counterstained with hematoxylin. The numbers of MMP9-expressing cells were counted on 5 randomly chosen fields from tumor and non-tumor areas in each animal at 400-fold magnification, by an examiner without any prior knowledge of the experimental procedures.

Cell proliferation assay

Human hepatoma-derived cell lines, HuH7 and HepG2 cells, were maintained in Dulbecco's modified essential medium (DMEM; Sigma chemical, St. Louis, MO) supplemented with 10% heat-inactivated fetal bovine serum (Atlanta Biological, Norcross, GA) in a humidified incubator at 37°C in 5% CO_2. HuH7 and HepG2 cells were seeded into each well of a 96-multi-well plate at a cell density of 1×10^4 and 5×10^3, respectively, in the presence of recombinant human CCL3 (R&D Systems) at different concentrations. Forty eight hours later, the cell viability was determined using WST-1 reagent (an MTT analog from Roche Diagnostics Corporation, Boehringer Mannheim) according to the manufacturer's instructions.

Enumeration of F4/80-positive cells

Paraffin-embedded sections were deparaffinized in xylene and rehydrated through graded concentrations of ethanol. After serial treatment with 1% (w/v) hydrogen peroxide in methanol, the sections were incubated overnight at 4°C with rat anti-mouse F4/80 (1 μg/ml) to detect macrophages/Kupffer cells. Tissue sections were then incubated with biotin-conjugated anti-rat immunoglobulin antibody and treated with a Catalyzed Signal Amplification Kit (DAKO) according to the manufacturer's instructions. The numbers of F4/80-positive cells were counted on 5 randomly chosen fields in tumor as well as non-tumor areas in each animal at 200-fold magnification, by an examiner without any prior knowledge of the experimental procedures. The area of each field is calculated to be 0.785 mm^2 and the numbers of F4/80-positive cells per mm^2 were calculated on both tumor and non-tumor areas.

CD34 immunohistochemical staining and intratumoral microvessel density determination

After deparaffinization of the sections, the slides were treated with 1% (w/v) hydrogen peroxide in PBS for 10 min and trypsin for 20 min at 37°C. Thereafter, the sections were incubated overnight at 4°C with 5 μg/ml of rat anti-mouse CD34 monoclonal antibody, to determine immunohistochemical staining and intratumoral microvessel density (IMVD).[24] Tissue sections were further incubated sequentially with biotin-conjugated anti-rat immunoglobulin antibody and ABC kit, according to the manufacturer's instructions. The slides were then reacted with a Vectastain DAB Substrate Kit and counterstained with hematoxylin. CD34-positive areas in the tumor tissues were defined as the intratumoral vascular areas. Fields of abundant neovascularization (hot spots) were found by scanning the sections at low magnification (×40 or ×100), and then the microvessel numbers as well as the pixel numbers of CD34-positive areas were determined on 5 randomly chosen fields in hot spots of each animal at 200-fold magnification, with the aid of Adobe Photoshop software Ver 7.0. IMVD was defined as the average number per one filed at 200-fold magnification and the percentage area of blood vessels.

Semi-quantitative reverse transcription (RT)-polymerase chain reaction (PCR)

Total RNA was extracted from a part of liver with RNAzol B, according to the manufacturer's instructions. After the RNA preparations were further treated with ribonuclease-free deoxyribonuclease (DNase) I (Life Technologies, Gaithersburg, MD) to remove residual genomic DNA, cDNA was synthesized as described previously.[11] Serially 2-fold diluted cDNA was amplified for β-actin, using specific sets of primers (Table I) as described previously.[11] Thereafter, equal amounts of cDNA products were amplified for cytokines, matrix metalloproteinases (MMP) and tissue inhibitors of MMP (TIMP), using specific sets of primers based on the reported sequences (Table I), with the indicated cycle numbers of 94°C for 30 sec, 55°C for 1 min and 72°C for 1 min. The amplified PCR products were fractionated on a 1.5% agarose gel and visualized by ethidium bromide staining. The intensities of the bands were measured with the aid of NIH Image Analysis software, and the ratios to β-actin were determined.

Statistical analysis

Tumor incidence was analyzed by using χ^2 test for contingency table. All other data were analyzed statistically using one-way ANOVA followed by the Fisher's protected least significance difference test or Mann–Whitney's U test. $p < 0.05$ was considered as statistically significant.

TABLE I – THE SEQUENCES OF THE PRIMERS AND THE CONDITIONS USED FOR RT-PCR ANALYSIS

	Sense primer	Antisense primer	Cycles	Product (bp)
β-*actin*	TGTGATGGTGGGAATGGGTCAG	TTTGATGTCACGCACGATTTCC	25	514
CCR1	TTTTAAGCCCCAGTGGGACTT	TGCTATAGCCACATGCCTTT	32	475
CCL3	ATCATGAAGGTCTCCACCAC	TCTCAGGCATTCAGTTCCAG	32	284
VEGF	CTGCTGTACCTCCACCATGCCAAGT	CTGCAAGTACGTTCGTTTAACTCA	35	509
bFGF	ACACGTCAAACTACAACTCCA	TCAGCTCTTAGCAGCACATTGG	35	295
HGF	GCTTGGCATCCACGATGTTC	CCCTCACATGGTCCTGATCC	35	387
Flt-1	TTAGGGGGTTCTCCATACCC	TATCTTCATGGAGGGCTTGG	35	531
Flk-1	CAGCTTCCAAGTGGCTAAGG	CATAATGGAATTTGGGGTCG	35	620
MMP2	GAGTTGGCACTGCAATACCT	GCGGTCCTTCTCAAAGTTGT	35	666
MMP9	AGTTTGCTGTCGCGGAGCAC	TACATGAGCGCTTCCGCCAC	35	754
MMP13	CTGGTCTTCTGGCACACGCT	GCAGCGCTCAGTCTCTTCAC	35	610
TIMP-1	CTGGCATCCTCTTGTTGCTA	AGGGATCTCCAGGTGCACAA	35	583
TIMP-2	AGACGTAGTGATCAGGGCCA	GTACCACGCGCAAGAACCAT	35	490

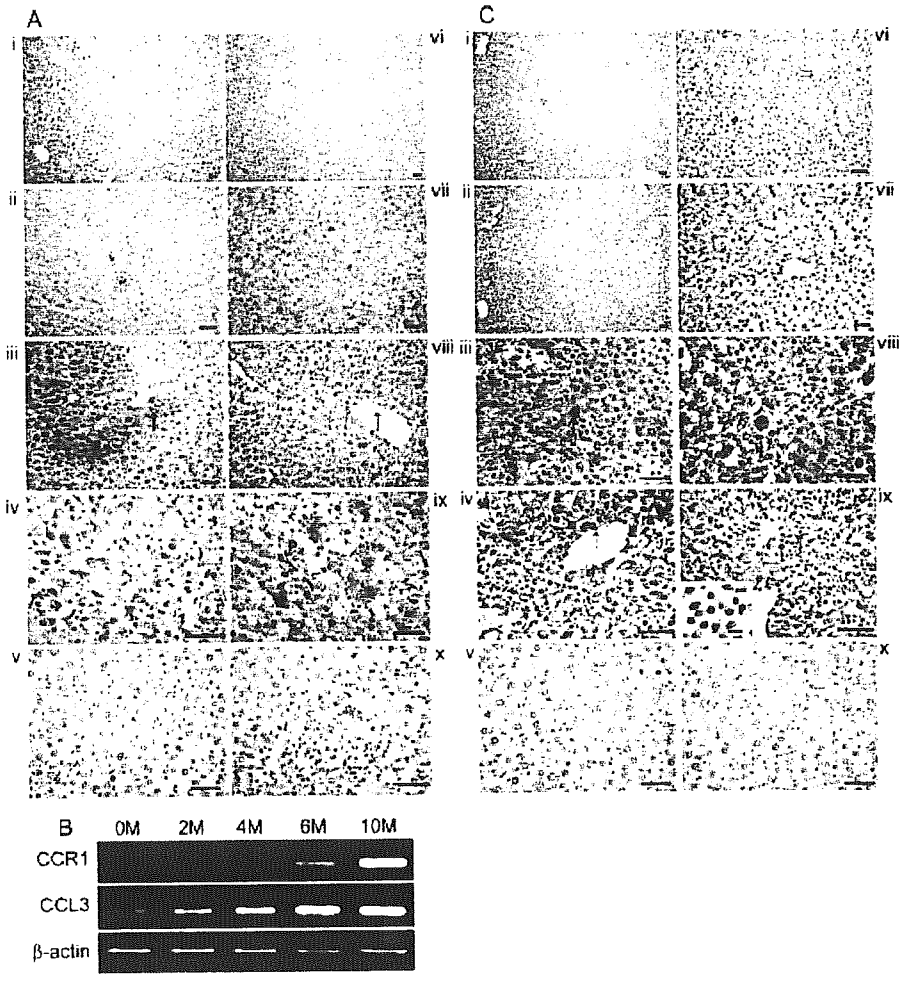

FIGURE 1 – Aberrant expression of CCR1 and CCL3 in hepatocarcinogenesis. (*a*) Immunohistochemical detection of CCR1 and CCL3 in HBs antigen transgenic mice. Immunohistochemical analysis using anti-CCR1 (*i–iv*), anti-CCL3 antibodies (*vi–ix*) or species-matched control antibodies (*v*, *x*) was performed on control liver (*i*, *vi*) and non-tumor (*ii*, *vii*) and tumor portions (*iii*, *iv*, *v*, *viii*, *ix* and *x*) in liver in HBs antigen transgenic mice at 15 months after splenocyte transfer, as described in Material and Methods. Representative results from 3 individual animals are shown here. The arrows in *iii* and *viii* indicate positively-stained bile duct and endothelial cells. *iv* and *ix* indicate positively-stained HCC cells. Original magnification, ×100 (*i* and *vi*), ×200 (*ii*, *iii*, *vii* and *viii*), ×400 (*iv*, *v*, *ix* and *x*). Scale bars, 50 μm. (*b*) *CCR1* and *CCL3* mRNA expression in liver after DEN treatment. RT-PCR was performed on total RNA extracted from WT mice liver at 0, 2, 4, 6, and 10 months after DEN treatment, as described in Material and Methods. Representative results from 5 individual experiments are shown here. (*c*) Immunohistochemical analysis of CCR1 and CCL3 protein in WT mice liver after DEN treatment. Liver tissues were obtained from WT mice at 2 (*i* and *vi*), 6 (*ii* and *vii*) and 10 months after DEN treatment (*iii*, *iv*, *v*, *viii*, *ix* and *x*). Immunohistochemical analysis was performed using anti-CCR1 (*i–iv*), anti-CCL3 antibodies (*vi–ix*) or species-matched control antibodies (*v*, *x*), as described in Material and Methods. Arrows in *iii* and *viii* indicate positively-stained HCC cells while an arrow in *iv* indicates positively-stained endothelial cells. The arrows and the inset (scale bar, 10 μm) in *ix* indicate infiltrating lymphocytes. Representative results from 3 animals from each time point are shown here. Original magnification, ×100 (*i* and *ii*), ×200 (*vi* and *vii*), ×400 (*iii*, *v* and *viii*–*x*). Scale bars, 50 μm.

Results

CCL3 and CCR1 expression was enhanced progressively in 2 mouse models of HCC development

We previously observed the constitutive expression of both CCL3 and its receptor, CCR1, in human HCC tissues.[11] Hence, to investigate the role of the CCL3-CCR1 axis in the HCC development, we first examined whether CCL3 and CCR1 proteins were expressed in mouse HCC arising in HBs antigen transgenic mice. We failed to detect any CCL3 and CCR1 protein expression in control mouse liver (Fig. 1*a-i* and *vi*). At 15 months after the HBs antigen-immunized splenocyte transfer, the liver possessed tumor areas surrounded by non-tumor areas, as described previously.[22] In non-tumor portions, a small number of hepatocytes were immunostained with anti-CCR1 (Fig. 1*a-ii*) or anti-CCL3 antibodies (Fig. 1*a-vii*). In contrast, tumor cells, some small bile duct cells and endothelial cells were strongly stained with anti-CCR1 or CCL3 antibodies (Fig. 1*a-iii*, *iv*, *viii* and *ix*). We next examined the expression patterns of CCL3 and CCR1 in mouse HCC induced by a chemical carcinogen, DEN. *CCL3* mRNA expression was faintly detected in liver from untreated WT mice, and enhanced progressively, thereafter. In contrast, *CCR1* gene expression was first detected 4 months after the treatment and was augmented progressively, thereafter (Fig. 1*b*). CCL3 protein was detected immunohistochemically occasionally on vascular endothelial cells in untreated mouse liver with no CCR1 expression (data not shown). Later than 2 months after DEN treatment, CCL3 protein was detected additionally in hepatocytes (Fig. 1*c-vi* and *vii*). At 10 months, CCL3 was evident in tumor cells (Fig. 1*c-viii*) and endothelial cells and some infiltrating mononuclear cells (Fig. 1*c-ix*). Concomitantly, CCR1 protein was expressed in tumor cells, vascular endothelial cells and some infiltrating mononuclear cells (Fig. 1*c-iii* and *iv*). Thus, CCR1 and CCL3 were aberrantly expressed in liver in both hepatocarcinogenesis models.

Effects of CCL3 on human hepatoma cell lines

Because CCR1 was expressed by hepatoma cells in both mouse and human,[11] we next evaluated the effects of CCL3 on human hepatoma cell lines. CCL3 inhibited the proliferation of human hepatoma cell lines marginally, but significantly, at concentrations higher than 100 ng/ml (Fig. 2*a* and 2*b*). Because hepatoma cells could produce CCL3 abundantly only in response to interleukin 1 and other pro-inflammatory cytokines but not constitutively,[11] CCL3 may have some autocrine and paracrine effects on hepatoma cells.

Important roles of the CCR1-CCL3 axis to DEN-induced hepatocarcinogenesis

To evaluate the contribution of CCR1 or CCL3 to DEN-induced hepatocarcinogenesis, we administered DEN to WT, CCR1-deficient and CCL3-deficient mice. At 10 months after DEN treatment, there was a marginal, but significant, difference in terms of HCC incidence between CCR1- and CCL3-deficient mice, compared with that of WT mice (5/13 cases, WT mice: 7/10, CCL3-deficient mice: 12/13, CCR1-deficient mice: $p < 0.05$). On the contrary, among tumor-bearing mice, the ratios of liver weights to body weights were significantly reduced in CCR1- and CCL3-deficient mice, compared with that of WT mice (Fig. 3*a*). Moreover, among tumor-bearing mice, the foci number per cm^2 and the proportion of tissues occupied with tumor were significantly decreased in CCL3- and to a lesser degree, CCR1-deficient mice, compared with that of WT mice (Fig. 3*b* and 3*c*). Since CCL3 can bind both CCR1 and CCR5,[1,2] the compensatory effect of CCR5 in CCR1-deficient mice may account for a lesser reduction in tumor numbers and sizes in CCR1- than CCL3-deficient mice. Nevertheless, these results suggest the important roles of the CCR1-CCL3 axis in DEN-induced hepatocarcinogenesis.

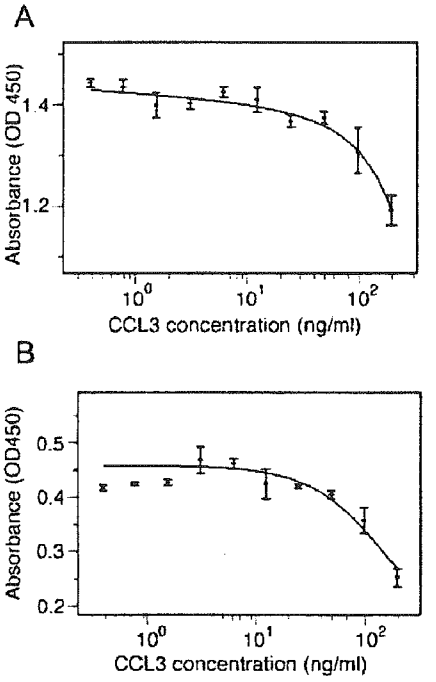

FIGURE 2 The effects of CCL3 on hepatoma cell lines. Either HuH7 (*a*) or HepG2 (*b*) cells were incubated in the presence of the indicated concentrations of CCL3, and cell proliferation rates were assessed as described in Material and Methods. Similar experiments were repeated 3 times and representative results are shown here with error bars as SEM ($n = 3$).

Reduced intratumoral neovascularization and Kupffer cell accumulation in DEN-treated CCR1- and CCL3-deficient mice

Reduced tumor foci number in CCR1- or CCL3-deficient mice may suggest that neovascularization, a prerequisite for hepatoma progression, was impaired in the absence of CCR1 or CCL3. Supporting this notion, both the microvessel numbers and the proportion of vascular areas in tumor areas were significantly reduced in CCL3- and CCR1-deficient mice, compared with WT mice (Fig. 4*a* and 4*b*). Because CCR1 is expressed by various types of cells including macrophages and Kupffer cells, a cellular source of various types of growth factors, we next determined macrophage and Kupffer cell numbers in HCC foci in WT and gene-deficient mice. In tumor areas, the numbers of F4/80-positive cells were remarkably depressed in both CCR1- and CCL3-deficient mice, compared with that of WT mice, although the numbers of F4/80-positive cells in non-tumor areas were only modestly reduced in CCL3- but not CCR1-deficient mice, compared with those of WT mice (Fig. 4*c*). Because F4/80 antigen is expressed by both Kupffer cells and blood-derived macrophages, a more specific marker for blood-derived macrophages, ER-MP20,[25] was used. However, we detected few, if any, ER-MP20-positive cells in this model (data not shown). These observations would indicate that the CCL3-CCR1 axis has a crucial role also in the accumulation of F4/80-positive Kupffer cells into tumor areas in this DEN-induced hepatocarcinogenesis.

Reduced MMP-9 expression in liver from DEN-treated CCR1- and CCL3-deficient mice

We next investigated the gene expression of potent angiogenic factors, vascular endothelial growth factor (VEGF), basic fibroblast growth factor (bFGF) and hepatocyte growth factor (HGF) by reverse transcription polymerase chain reaction (RT-PCR). The gene expression of these angiogenic factors did not change

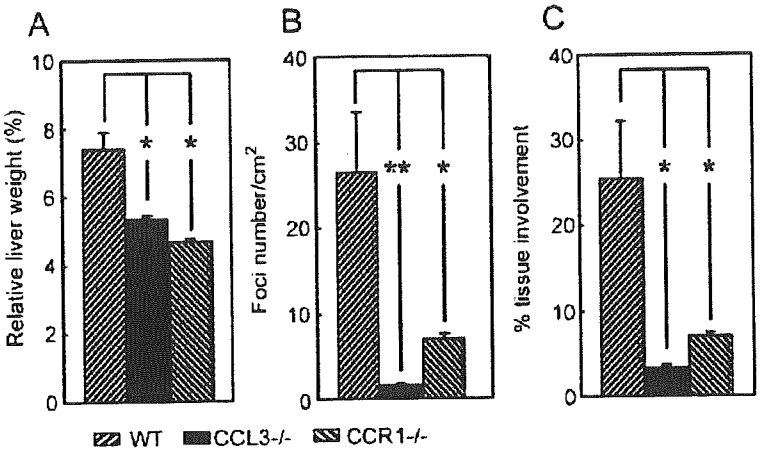

FIGURE 3 – Attenuated tumor formation in CCR1- and CCL3-deficient mice at 10 months after DEN treatment. Livers were obtained from mice at 10 months after DEN treatment to examine the presence of HCC foci. Among tumor-bearing mice of each strain (WT mice, $n = 5$; CCL3-deficient mice, $n = 7$; CCR1-deficient mice, $n = 12$), the relative ratios of liver to body weights (*a*), foci number per cm^2 (*b*), and the proportion of tissues occupied with tumor foci (*c*) were determined as described in Material and Methods. Each value represents mean ± SEM. * indicate $p < 0.05$, compared with that of WT mice.

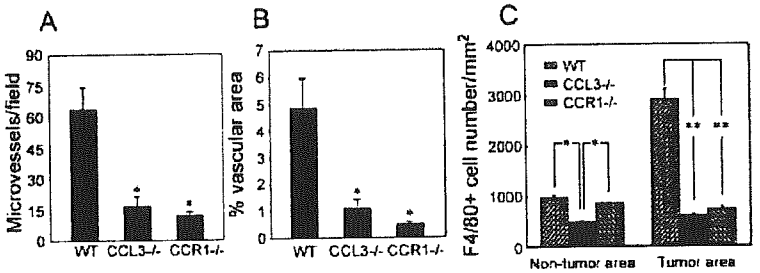

FIGURE 4 – Reduced IMVD and Kupffer cell numbers in liver of DEN-treated CCR1- and CCL3-deficient mice. (*a* and *b*) Livers were obtained from each strain at 10 months after DEN treatment and processed for immunostaining with anti-CD34 antibodies. IMVD was defined as the microvessel numbers per field at 200-fold magnification (*a*) or the proportions of CD34-positive areas (*b*) as described in Material and Methods, each value represents mean ± SEM ($n = 5$). * indicate $p < 0.05$, compared with that of WT mice. (*c*) Livers were obtained from each strain at 10 months after DEN treatment and processed for immunostaining with an anti-F4/80 monoclonal antibody. The numbers of F4/80-positive cells in non-tumor and tumor areas were determined as described in Material and Methods. Each value represents mean ± SEM ($n = 5$) *, $p < 0.05$; **, $p < 0.01$.

significantly in WT mice, at any time after DEN injection that we examined (Fig. 5*a*). Similar results were obtained for the expression of VEGF receptors, *Flk-1* and *Flt-1* (Fig. 5*a*). Moreover, there were no significant differences in terms of the expression of these factors and receptors between WT and CCL3- or CCR1-deficient mice (data not shown). Because the balance between MMP and TIMP has crucial roles in the degradation of extracellular matrix proteins and subsequent angiogenesis, we next determined the gene expression of MMP and TIMP. Among MMP and TIMP that we examined, *MMP9* and *MMP13* gene expression was augmented progressively in WT mouse liver after DEN treatment (Fig. 5*b*). Moreover, *MMP9*, but not *MMP13*, gene expression was remarkably reduced in CCL3- and CCR1-deficient mice, compared with that of WT mice (Fig. 5*c*). We further observed that MMP9 proteins were detected in mononuclear cells accumulated inside hepatoma tissues arising in both DEN-treated mice (Fig. 5*d*) and HBs antigen transgenic mice (data not shown). We cannot exclude completely the possibility that HCC cells express MMP9 below the detection limit of the present immunohistochemical analysis. Nevertheless, it is likely that a major source of MMP9 was mononuclear cells in these models. Moreover, the number of MMP9-positive cells in tumor sites were significantly decreased in CCR1- or CCL3-deficient mice, compared with that of WT mice (Fig. 5*d* and 5*e*).

Discussion

DEN, a potent chemical hepatocarcinogen, acts as an initiator to cause a G-C to A-T transition mutation through the methylation of guanine.[26] As a result, when suckling rodents were given DEN, HCC developed with a high frequency with minimal inflammatory changes.[15,16] Myelo-depleted HBs transgenic mice developed HCC until 15 months after the transfer of splenocytes obtained from syngeneic non-transgenic mice that had been primed with HBs antigen.[22] This hepatocarcinogenesis occurred in the presence of chronic hepatitis, as observed in human HCC associated with chronic HBV or HCV infection.[7] Here, we have provided definitive evidence that CCL3 and CCR1 were expressed aberrantly in tumor cells in these 2 distinctive murine hepatocarinogenesis models. Thus, together with our previous observations on human HCC tissues,[11] these results suggest the generality of the aberrant expression of CCR1 and CCL3 in HCC tissues.

To define the roles of the CCL3-CCR1 axis in hepatocarcinogenesis, we administered DEN to CCR1- and CCL3-deficient mice as well as WT mice. Interestingly, both CCL3 and CCR1 affected both HCC initiation and tumor progression, but in opposite ways. Whereas HCC occurred more frequently in both CCL3- and CCR1-deficient mice compared with that of WT controls, tumor burden (foci number and the proportion of the organ occupied by tumor) was dramatically reduced in the former mice. The precise mechanisms underlying these effects are not yet clear, however, our data point to several intriguing possibilities. With regard to disease initiation, we found that recombinant CCL3 stimulation of hepatoma cell lines is able to retard cell growth *in vitro* in a concentration dependent manner. *In vivo*, this could potentially translate into a growth disadvantage for newly transformed hepatocarcinoma cells, thereby, facilitating surveillance and eradication of these cells by immune-mediated mechanisms

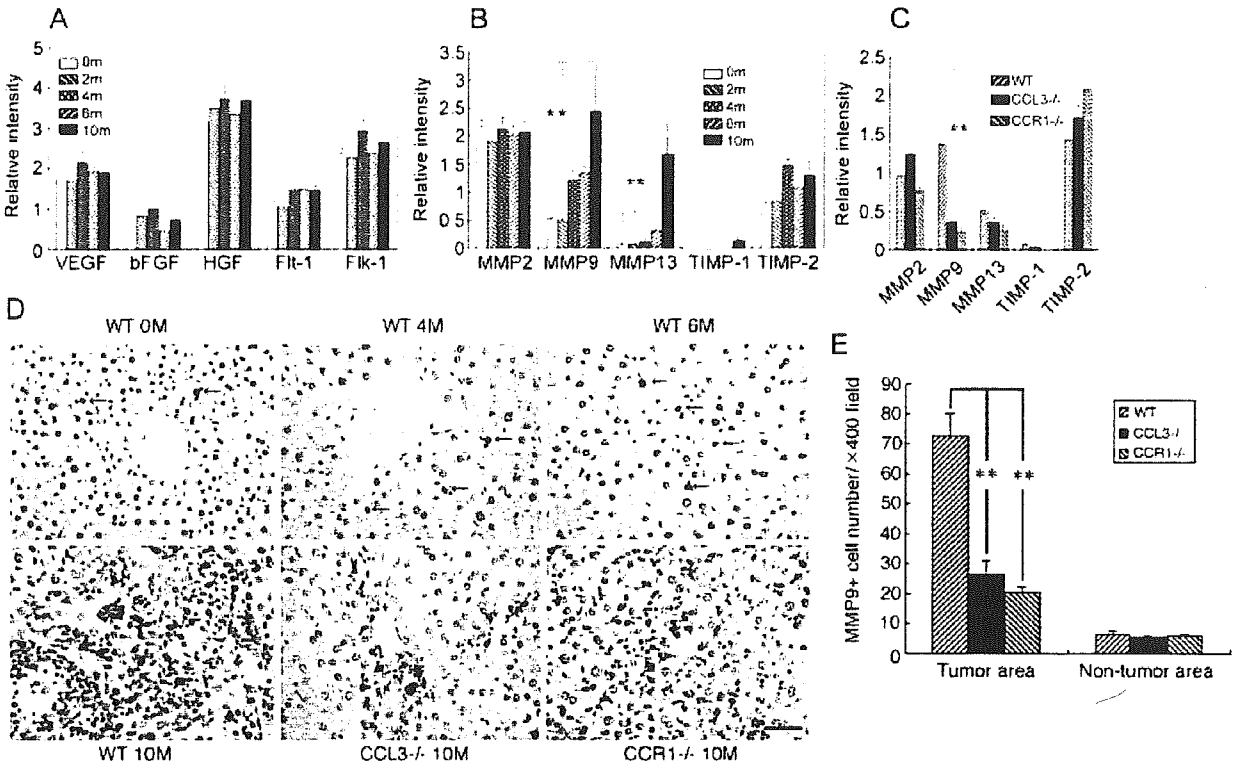

FIGURE 5 – (*a–c*) Gene expression of angiogenic factors and their receptors and matrix metalloproteinses. (*a*) RT-PCR for the genes of angiogenic factors and VEGF receptors was performed on total RNA extracted from WT mice liver at the indicated time intervals (0, 2, 4, 6 and 10 months) after DEN treatment, as described in Material and Methods. The ratios of each gene to β-actin were determined. Each value represents mean ± SEM ($n = 5$). m, month. (*b*) RT-PCR for MMP and TIMP genes was performed on total RNA extracted from WT mice liver at 0, 2, 4, 6 and 10 months after DEN treatment, as described in Material and Methods. The ratios of each gene to β-actin were determined. Each value represents mean ± SEM ($n = 5$) with ** indicating $p < 0.01$, compared with 0 month. m, month. (*c*) RT-PCR for the indicated genes was performed on total RNA extracted from tumor bearing liver of WT, CCR1- and CCL3-deficient mice at 10 months after DEN treatment in a separate experiment from the experiments shown in Figure 5*a* and *b*, as described in Material and Methods. The ratios of each gene to β-actin were determined. Each value represents mean ± SEM ($n = 5$) with ** indicating $p < 0.01$, compared with that of WT mice. (*d*) Immunohistochemical detection of MMP9-positive cells in liver after DEN treatment. Immunohistochemical analysis was performed on liver tissues obtained from WT, CCL3- or CCR1-deficient mice at the indicated time intervals after DEN treatment, as described in Material and Methods. Representative results from 6 individual animals are shown here. Original magnification, ×400. Scale bars, 50 μm. (*e*) The numbers of MMP9-positive cells in WT, CCL3- or CCR1-deficient mice liver at 10 months after DEN treatment. All values and bars represent the mean and SEM calculated on the results from 6 individual animals, respectively. **, $p < 0.01$.

The net result would be decreased incidence of HCC in WT mice as compared with those of CCL3- or CCR1-deficient mice.

Maeda and colleagues demonstrated that NF-κB activation in hepatocytes could be protective for DEN-induced hepatocarcinogenesis, while NF-κB activation in intrahepatic hematopoietic cells could promote it.[27] Evidence is accumulating to indicate that CCR1-mediated signal could activate NF-κB in several types of cells.[28,29] Moreover, we observed that CCR1 was expressed by hepatocytes and intrahepatic mononuclear cells. Thus, the net effects of the CCR1-CCL3 system may be a balance between its capacities to activate NF-κB in these 2 distinct types of cells. In the initial step when mononuclear cells were scarce in liver, the CCR1-CCL3 system may activate NF-κB, mainly in hepatocytes, which may account for a lower HCC incidence in WT mice than in CCR1- or CCL3-deficient mice. Our data indicate that CCL3 and CCR1 are important for mononuclear cell accumulation in tumor, consistent with their known chemotactic effects *in vitro* and that some of these cells express a major angiogenic factor, MMP9 whose gene expression can be induced by NF-κB activation.[30] Because angiogenesis is presumed to be crucially required for HCC progression,[31] these combined effects could be a major factor restricting the size of tumors in CCL3- and CCR1-deficient mice.

Although several lines of evidence implied VEGF as an essential mediator regulating hypervascularity in HCC,[32,33] we failed to detect any changes in VEGF and its receptor gene expression during the whole course of DEN-induced hepatocarcinogenesis. Moreover, we did not see any differences in VEGF and its receptor gene expression in liver between WT and either CCR1- or CCL3-deficient mice. Thus, it is unlikely that VEGF was a main mediator controlling angiogenesis in this model.

Evidence is accumulating to indicate that the balance between MMP and their inhibitors, TIMP, has crucial roles in tumor progression by inducing tumor angiogenesis and altering the extracellular environment more suitable for tumor cell establishment and growth.[34] Moreover, several cDNA microarray analyses on human HCC have revealed that the expression of some MMPs were enhanced in HCC tissues, compared with that of non-tumor portion.[35,36] These observations prompted us to examine MMP and TIMP gene expression by RT-PCR analysis. Among MMPs and TIMPs that we examined, only *MMP9* and *MMP13* gene expression were augmented progressively after DEN treatment, and *MMP9*, but not *MMP13*, gene expression was significantly attenuated in liver of DEN-treated CCR1- and CCL3-deficient mice, compared with that of WT mice. Crucial involvement of MMP9 in angiogenesis has been substantiated by the observations on

MMP9-deficient mice.[37] Moreover, MMP9-positive cells appeared even in premalignant lesion in the absence of neovascularization (our unpublished data), and MMP9-positive cell numbers in tumor areas were significantly reduced in CCR1- or CCL3-deficient mice, compared with that in WT mice. Thus, it is likely that the reduction in MMP9 expression can account for attenuated tumor angiogenesis in CCR1- and CCL3-deficient mice.

Several lines of evidence indicate that bone marrow-derived progenitors can direct neovascularization.[38,39] Moreover, CCL3 exhibits a potent mobilizing activity for hematopoietic stem cells[40] by predominantly interacting with CCR1.[41] Furthermore, MMP9 was required for hematopoietic stem cell mobilization from bone marrow to other organs, including liver.[42,43] We also detected the presence of c-kit-positive stem cells co-expressing CCR1 in the tumor foci of DEN-treated, but not untreated, WT mice (our unpublished data). Thus, it is tempting to speculate that HCC-derived CCL3 induced hematopoietic stem cell mobilization into liver, in collaboration with MMP9 and that hematopoietic stem cells can induce tumor angiogenesis, in concert with MMP9.

Several gene loci, which have been identified as the loci determining the sensitivity of hepatocytes to DEN, are localized on mouse chromosomes 1, 2, 7, 8 and 12.[44] The present results suggest that both CCR1 and CCL3 have profound effects on the progression of DEN-induced hepatocarcinogenesis. Because *CCR1* and *CCL3* genes are localized on mouse chromosomes 9 and 11, respectively, these genes must be hitherto unidentified genes that determine the sensitivity to DEN-induced hepatocarcinogenesis. Moreover, given that both CCL3 and CCR1 were expressed by HCC cells, it is likely that the CCL3-CCR1 axis has some direct effects on HCC cells and can eventually regulate HCC progression induced by DEN treatment. Furthermore, aberrant expression of CCL3 and CCR1 was also observed in human HCC tissues[11] as well as in our murine hepatocarcinoma models in DEN-treated mice and HBs transgenic mice. Thus, CCL3 and CCR1 may be involved in the progression of HCC in general. If so, detailed molecular analysis on DEN-treated CCL3- or CCR1-deficient mice will shed a novel light on the molecular pathogenesis of HCC.

Acknowledgements

We thank Drs. T. Kondo, Y. Ishida (Department of Legal Medicine, Wakayama Medical University), T. Irimura, K. Denda-Nagai (Graduate School of Pharmaceutical Sciences, University of Tokyo), and M. Naito (Graduate School of Medical and Dental Sciences, Niigta University) for their invaluable advice on the immunostaining.

References

1. Baggiolini M. Chemokines and leukocyte traffic. Nature 1998;392:565–8.
2. Luster AD. Chemokines-chemotactic cytokines that mediate inflammation. N Engl J Med 1998;338:436–45.
3. Premack BA, Schall TJ. Chemokine receptors: gateways to inflammation and infection. Nat Med 1996;2:1174–8.
4. Brault MS, Kurt RA. Chemokines and antitumor immunity: walking the tightrope. Int Rev Immunol 2003;22:199–28.
5. Bernardini G, Ribatti D, Spinetti G, Morbidelli L, Ziche M, Santoni A, Capogrossi MC, Napolitano M. Analysis of the role of chemokines in angiogenesis. J Immunol Methods 2003;273:83–101.
6. Homey B, Muller A, Zlotnik A. Chemokines: agents for the immunotherapy of cancer? Nat Rev Immunol 2002;2:175–84.
7. Sell S. Mouse models to study the interaction of risk factors for human liver cancer. Cancer Res 2003;63:7553–62.
8. Mahe Y, Mukaida N, Kuno K, Akiyama M, Ikeda N, Matsushima K, Murakami S. Hepatitis B virus X protein transactivates human interleukin-8 gene through acting on nuclear factor κB and CCAAT/enhancer-binding protein-like cis-elements. J Biol Chem 1991;266:13759–63.
9. Polyak SJ, Khabar KS, Paschal DM, Ezelle HJ, Duverlie G, Barber GN, Levy DE, Mukaida N, Gretch DR. Hepatitis C virus nonstructural 5A protein induces interleukin-8, leading to partial inhibition of the interferon-induced antiviral response. J Virol 2001;75:6095–106.
10. Iguchi A, Kitajima I, Yamakuchi M, Ueno S, Aikou T, Kubo T, Matsushima K, Mukaida N, Maruyama I. PEA3 and AP-1 are required for constitutive IL-8 gene expression in hepatoma cells. Biochem Biophys Res Commun 2000;279:166–71.
11. Lu P, Nakamoto Y, Nemoto-Sasaki Y, Fujii C, Wang H, Hashii M, Ohmoto Y, Kaneko S, Kobayashi K, Mukaida N. Potential interaction between CCR1 and its ligand, CCL3, induced by endogenously produced interleukin-1 in human hepatomas. Am J Pathol 2003;162:1249–58.
12. Geller SA. Hepatitis B and hepatitis C. Clin Liver Dis 2002;6:317–34.
13. Chen CJ, Chen DS. Interaction of hepatitis B virus, chemical carcinogen, and genetic susceptibility: multistage hepatocarcinogenesis with multifactorial etiology. Hepatology 2002;36:1046–9.
14. Berger MR, Schmahl D, Edler L. Implications of the carcinogenic hazard of low doses of three hepatocarcinogenic A nitrosamines. Jpn J Cancer Res 1990;81:598–606.
15. Yang X, Bhaumik M, Bhattacharyya R, Gong S, Rogler CE, Stanley P. New evidence for an extra-hepatic role of *N*-acetylglucosaminyltransferase III in the progression of diethylnitrosamine-induced liver tumors in mice. Cancer Res 2000;60:3313–9.
16. Lee YS, Kim WH, Yu ES, Kim MR, Lee MJ, Jang JJ. Time course of cell cycle-related protein expression in diethylnitrosamine-initiated rat liver. J Hepatol 1998;29:464–9.
17. Tokuda A, Itakura M, Onai N, Kimura H, Kuriyama T, Matsushima K. Pivotal role of CCR1-positive leukocytes in bleomycin-induced lung fibrosis in mice. J Immunol 2000;164:2735–51.
18. Cook DN, Beck MA, Coffman TM, Kirby SL, Sheridan JF, Pragnell IB, Smithies O. Requirement of MIP-1 α for an inflammatory response to viral infection. Science 1995;269:1583–5.
19. Gao JL, Wynn TA, Chang Y, Lee EJ, Broxmeyer HE, Cooper S, Tiffany HL, Westphal H, Kwon-Chung J, Murphy PM. Impaired host defense, hematopoiesis, granulomatous inflammation and type 1-type 2 cytokine balance in mice lacking CC chemokine receptor 1. J Exp Med 1997;185:1959–68.
20. Chisari FV, Filippi P, McLachlan A, Milich DR, Riggs M, Lee S, Palmiter RD, Pinkert CA, Brinster RL. Expression of hepatitis B virus large envelope polypeptide inhibits hepatitis B surface antigen secretion in transgenic mice. J Virol 1986;60:880–7.
21. Nakano H, Hatayama I, Satoh K, Suzuki S, Sato K, Tsuchida S. c-Jun expression in single cells and preneoplastic foci induced by diethylnitrosamine in B6C3F1 mice: comparison with the expression of pi-class glutathione S-transferase. Carcinogenesis 1994;15:1853–7.
22. Nakamoto Y, Guidotti LG, Kuhlen CV, Fowler P, Chisari FV. Immune pathogenesis of hepatocellular carcinoma. J Exp Med 1998;188:341–50.
23. Pierce RH, Vail ME, Ralph L, Campbell JS, Fausto N. Bcl-2 expression inhibits liver carcinogenesis and delays the development of proliferating foci. Am J Pathol 2002;160:1555–60.
24. Martin L, Green B, Renshaw C, Lowe D, Rudland P, Leinster SJ, Winstanley J. Examining the technique of angiogenesis assessment in invasive breast cancer. Brit J Cancer 1997;76:1046–54.
25. Leenen PJ, Melis M, Slieker WA, Van Ewijk W. Murine macrophage precursor characterization. II. Monoclonal antibodies against macrophage precursor antigens. Eur J Immunol 1990;20:27–34.
26. Nakatsuru Y, Matsukuma S, Nemoto N, Sugano H, Sekiguchi M, Ishikawa T. O_6-methylguanine-DNA methyltransferase protects against nitrosamine-induced hepatocarcinogenesis. Proc Natl Acad Sci USA 1993;90:6468–72.
27. Maeda S, Kamata H, Luo JL, Leffert H, Karin M. IKKβ couples hepatocytes death to cytokine-driven compensatory proliferation that promotes chemical hepatocarcinogenesis. Cell 2005;121:977–90.
28. Omoike OI, Teague RM, Benedict SH, Chan MA. MIP-1α induces binding of nuclear factors to the κB DNA element in human B cells. Mol Cell Biol Res Commun 2000;4:15–9.
29. Ness TL, Carpenter KJ, Ewing JL, Gerard CJ, Hogaboam CM, Kunkel SL. CCR1 and CC chemokine ligand 5 interactions exacerbate innate immune response during sepsis. J Immunol 2004;173:6938–48.
30. Xie Z, Singh M, Singh K. Differential regulation of matrix metalloproteinase 2 and -9 expression and activity in adult rat cardiac fibroblasts in response to interleukin-1β. J Biol Chem 2004;279:39513–9.
31. Okuda K. Early recognition of hepatocellular carcinoma. Hepatology 1986;6:729–38.
32. Mise M, Arii S, Higashitsuji H, Furutani M, Niwano M, Harada T, Ishigami S, Toda Y, Nakayama H, Fukumoto M, Fujita J, Imamura M. Clinical significance of vascular endothelial growth factor and basic fibroblast growth factor gene expression in liver tumor. Hepatology 1996;23:455–64.

33. Miura H, Miyazaki T, Kuroda M, Oka T, Machinami R, Kodama T, Shibuya M, Makuuchi M, Yazaki Y, Ohnishi S. Increased expression of vascular endothelial growth factor in human hepatocellular carcinoma. J Hepatol 1997;27:854–61.
34. John A, Tuszynski G. The role of matrix metalloproteinases in tumor angiogenesis and tumor metastasis. Pathol Oncol Res 2001;7:14–23.
35. Okabe H, Satoh S, Kato T, Kitahara O, Yanagawa R, Yamaoka Y, Tsunoda T, Furukawa Y, Nakamura Y. Genome-wide analysis of gene expression in human hepatocellular carcinomas using cDNA microarray: identification of genes involved in viral carcinogenesis and tumor progression. Cancer Res 2001;61:2129–37.
36. Chen X, Cheung ST, So S, Fan ST, Barry C, Higgins J, Lai K-M, Ji J, Dudoit S, Ng IOL, van deRijn M, Botstein D, Brown PO. Gene expression patterns in human liver cancers. Mol Biol Cell 2002;13:1929–39.
37. Vu TH, Shipley JM, Bergers G, Berger JE, Helms JA, Hanahan D, Shapiro SD, Senior RM, Werb Z. MMP-9/gelatinase B is a key regulator of growth plate angiogenesis and apoptosis of hypertrophic chondrocytes. Cell 1998;93:411–22.
38. Bagley RG, Walter-Yohrling J, Cao X, Weber W, Simons B, Cook BP, Chartrand SD, Wang C, Madden SL, Teicher BA. Endothelial precursor cells as a model of tumor endothelium: characterization and comparison with mature endothelial cells. Cancer Res 2003;63:5866–73.
39. Takakura N, Watanabe T, Suenobu S, Yamada Y, Noda T, Ito Y, Satake M, Suda T. A role for hematopoietic stem cells in promoting angiogenesis. Cell 2000;102:199–209.
40. Lord BI, Woolford LB, Wood LM, Czaplewski LG, McCourt M, Hunter MG, Edwards RM. Mobilization of early hematopoietic progenitor cells with BB-10010: a genetically engineered variant of human macrophage inflammatory protein-1α. Blood 1995;85:3412–5.
41. Broxmeyer HE, Cooper S, Hangoc G, Gao JL, Murphy PM. Dominant myelopoietic effector functions mediated by chemokine receptor CCR1. J Exp Med 1999;189:1987–92.
42. Kollet O, Shivtiel S, Chen YQ, Suriawinata J, Thung SN, Dabeva MD, Kahn J, Spiegel A, Dar A, Samira S, Goichberg P, Kalinkovich A, et al. HGF, SDF-1, and MMP-9 are involved in stress-induced human CD34$^+$ stem cell recruitment to the liver. J Clin Invest 2003;112:160–9.
43. Heissig B, Hattori K, Dias S, Friedrich M, Ferris B, Hackett NR, Crystal RG, Besmer P, Lyden D, Moore MA, Werb Z, Rafii S. Recruitment of stem and progenitor cells from the bone marrow niche requires MMP-9 mediated release of kit-ligand. Cell 2002;109:625–37.
44. Gariboldi M, Manenti G, Canzian F, Falvella FS, Pierotti MA, Della Porta G, Binelli G, Dragani TA. Chromosome mapping of murine susceptibility loci to liver carcinogenesis. Cancer Res 1993;53:209–11.

CLINICAL GASTROENTEROLOGY AND HEPATOLOGY 2005;3:1253–1259

Pretreatment Prediction of Interferon-Alfa Efficacy in Chronic Hepatitis C Patients

KAZUHIRO HAYASHIDA,* AKITO DAIBA,† AKITO SAKAI,§ TAKESHI TANAKA,¶ KYOSUKE KAJI,§ NIRO INABA,† SATOSHI ANDO,† NAOKI KAJIYAMA,† HIROSHI TERASAKI,† AKI ABE,† MASANORI OGASAWARA,† MICHINORI KOHARA,‖ MINE HARADA,* TAKESHI OKANOUE,# SATORU ITO,† and SHUICHI KANEKO§

*Medicine and Biosystemic Science, Kyushu University Graduate School of Medical Sciences, Higashi-ku, Fukuoka, Japan; †JGS Japan Genome Solutions, Inc., Hachioji, Tokyo, Japan; §Kanazawa University Graduate School of Medical Sciences, Kanazawa, Japan; ¶Tokyo Metropolitan Komagome Hospital, Bunkyo-ku, Tokyo, Japan; ‖Tokyo Metropolitan Institute of Medical Science, Bunkyo-ku, Tokyo, Japan; #Kyoto Prefectural University of Medicine, Graduate School of Medical Science, Kawaramachi-Hirokoji, Kamigyo-ku, Kyoto, Japan

Background & Aims: Interferon has been used widely to treat patients with chronic hepatitis C infections. Prediction of interferon efficacy before treatment has been performed mainly by using viral information, such as viral load and genotype. This information has allowed the successful prediction of sustained responders (SR) and non-SRs, which includes transient responders (TR) and nonresponders (NR). In the current study we examined whether liver messenger RNA expression profiles also can be used to predict interferon efficacy. *Methods:* RNA was isolated from 69 liver biopsy samples from patients receiving interferon monotherapy and was analyzed on a complementary DNA microarray. Of these 69 samples, 31 were used to develop an algorithm for predicting interferon efficacy, and 38 were used to validate the precision of the algorithm. We also applied our methodology to the prediction of the efficacy of interferon/ribavirin combination therapy using an additional 56 biopsy samples. *Results:* Our microarray analysis combined with the algorithm was 94% successful at predicting SR/TR and NR patients. A validation study confirmed that this algorithm can predict interferon efficacy with 95% accuracy and a *P* value of less than .00001. Similarly, we obtained a 93% prediction efficacy and a *P* value of less than .0001 for patients receiving combination therapy. *Conclusions:* By using only host data from the complementary DNA microarray we are able to successfully predict SR/TR and NR patients for interferon therapy. Therefore, this technique can help determine the appropriate treatment for hepatitis C patients.

Chronic hepatitis C is one of the major causes of chronic liver disease and can lead to cirrhosis and hepatocellular carcinoma. Interferon is the only effective drug for chronic hepatitis C patients, although better efficacy can be attained with modification of the regimen including the amount of interferon, the duration of treatment, and the use of a combination of pegylated-interferon and ribavirin.

Many studies have identified factors that can help predict the efficacy of interferon therapy such as hepatitis C virus (HCV) genotype[1] and viral loads.[2] Methods based on viral information are able to identify sustained responders (SR). However, this method places transient responders (TR) and nonresponders (NR) in the same category. Follow-up data clearly indicate that interferon treatment of patients in the TR group can lead to a reduction in the probability of tumor development compared with the NR group.[3,4] This suggests that the NR patients should be separated out first and that the TR group should be handled separately as an SR-like group. Furthermore, host factors may help the prediction of NR clinical outcome before treatment. Several candidates have been suggested that may be used to predict this effect including body mass index,[5] γ-glutamyltransferase/alanine transaminase levels,[6] the messenger RNA expression levels of the interferon receptor,[7,8] interferon-γ and tumor necrosis factor-α levels,[9] and the Th1/Th2 ratio[10]; however, there is no definitive evidence that any of these is a single dominant factor. Therefore, additional studies must be performed to identify host factors that can predict the efficacy of interferon therapy because complex changes in these host parameters may reflect variations in hepatic gene expression.

Complementary DNA (cDNA) microarrays can provide an enormous amount of data for identifying clusters

Abbreviations used in this paper: cDNA, complementary DNA; HCV, hepatitis C virus; MD, Mahalanobis distance; NR, nonresponder; SR, sustained responder; SSDB, standard space database; TR, transient responder.

© 2005 by the American Gastroenterological Association

1542-3565/05/$30.00
PII: 10.1053/S1542-3565(05)00412-X

of predictive factors. For example, we previously have used custom-made cDNA microarrays to dissect gene expression patterns and to differentiate between patients infected with HCV and hepatitis B virus.[11,12] Other oligo-DNA chip approaches have proven to be very effective for identifying sets of genes expressed in vitro in response to interferon.[13] However, these approaches have not been useful for determining which treatment regimen should be used for each patient. In the current study we developed a cDNA microarray and a data analysis algorithm that can predict whether a patient will be an NR for interferon therapy based only on host messenger RNA expression and without the use of viral data.

Materials and Methods

Patients and Biopsy Samples

From 1993 to 2001, we collected liver biopsy samples from 99 HCV patients undergoing interferon monotherapy at Kyushu University Hospital. In addition, between 1999 and 2002, an additional 4 samples were collected from patients undergoing interferon monotherapy at Kanazawa University Hospital and 5 samples from Kyoto Prefectural University Hospital as part of a validation study. These patients received the standard 6-month protocol for interferon-alfa treatment. Thus, all patients received more than 468 MU of interferon-alfa monotherapy. Finally, between 2002 and 2003, 56 patients at Kanazawa University Hospital and Tokyo Metropolitan Komagome Hospital were treated with a 6-month regimen of interferon-alfa combined with 600–800 mg/day of ribavirin. Informed consent was obtained from all patients in accordance with the Helsinki protocol. Liver samples were obtained from these patients by biopsy procedure with a 14- or 16-gauge needle. The samples were snap-frozen in liquid nitrogen and stored at −80°C until use for RNA extraction. The viral genotype in pretreatment serum samples from these patients was determined as described previously,[14] the viral RNA copy number was tested using the HCV Amplicore kit (Roche Japan, Tokyo, Japan), and the viral serotype was assayed using an F-HCV-Gr enzyme-linked immunosorbent assay kit (Sysmex, Kobe, Japan). The patients were categorized into 3 groups: SR (patients with an absence of serum HCV RNA both during therapy and 6 months after the completion of therapy), NR (patients persistently positive for serum HCV RNA during therapy), and TR (patients negative for serum HCV RNA at the end of interferon treatment but positive after cessation of therapy).

RNA Extraction, Complementary DNA Microarray, Data Collection, and Data Mining

The total RNA extraction procedure from biopsy samples and the low-density cDNA microarray together with a unique artificial reference RNA (Genomessage; JGS, Tokyo, Japan) used in these studies were described in our previous report.[15]

Results

Selection of Liver Biopsy Samples

RNA degradation is one of the main factors causing variability in data from cDNA microarrays. Because some of the biopsy samples used in this study were stored for more than 8 years, we examined the quality of the extracted RNA by microcapillary electrophoresis. Enough RNA (>2 μg) was obtained from only 69 of the 108 samples from patients treated with interferon monotherapy. We randomly divided these 69 samples into 2 groups of 31 and 38 samples for training and validation of the prediction algorithm, respectively. Based on the 28S/18S ratio, the RNA quality of these 69 samples was good. Of the 69 total patients, 47 were men and 22 were women, and the average age was 49 ± 12 years (range, 21–71 y). Table 1 summarizes the values of alanine transaminase, γ-glutamyltransferase, viral load, and genotypes for the 31 samples used for developing the prediction algorithm. Similarly, qualified RNA extracted from all 56 samples that had been obtained from patients receiving combination therapy were divided randomly into 2 groups of 33 and 23 samples. Of these patients, 46 were men and 10 were women, and the average age was 54 ± 8 years (range, 39–71 y). The characteristics of the group of 33 patients for establishment of SSDB are summarized in Table 2.

Development of the Complementary DNA Microarray

To develop the cDNA microarray for the current study we first performed a serial analysis of gene expression on data from normal and hepatitis B and C patients for approximately 2000 genes. For this serial analysis of gene expression study we analyzed the results from our previous microarray analysis combined with publicly available data.[16,17] During this initial screening phase we tried to choose genes that could distinguish between hepatitis and normal samples. In addition, to focus on genes with meaningful signal levels, we omitted those with a low-frequency expressed tag in serial analysis of gene expression. These approaches are consistent with those of Chang et al[18] who, for statistical calculation, selected only the strong intensity signals from their GeneChip (Affymetrix; Santa Clara, CA) data. Furthermore, we omitted most sequences representing expressed sequence tags in the serial analysis of gene expression data. Finally, we selected genes whose functions have been well established. For example, 26 interferon-related genes were selected for the microarray. We also tried to select genes that have been reported previously to predict interferon efficacy, including interferon-alfa/β receptor,

Table 1. Characteristics of the Core Patients Used for the SSDB and Training

Number	Age	Sex	Genotype	Viral load (*KIU/mL*)	Histology/stage and activity	ALT (*IU/L*)	γ-GT (*IU/L*)	Clinical outcome	Use
1	23	F	1b	4.4	F1A1	90	32	SR	SSDB
2	31	M	2a	23	F1A1	29	11	SR	SSDB
3	34	F	2a	3.5	F1A1	32	199	SR	SSDB
4	40	M	2a	100	F1A2	233	68	SR	SSDB
5	41	M	1b	110	F1A2	182	117	SR	SSDB
6	48	M	2a	2.2	F2A2	189	37	SR	SSDB
7	50	M	2b	3.7	F1A3	267	114	SR	SSDB
8	54	F	2a	2.3	F1A2	41	31	SR	SSDB
9	55	M	2a	2.4	F1A1	301	85	SR	SSDB
10	58	M	1b	50	F1A2	36	59	SR	SSDB
11	60	M	2b	50	F1A1	149	150	SR	SSDB
12	66	M	2a	1.8	F3A2	286	104	SR	SSDB
13	66	M	1b	140	F1A1	88	31	SR	SSDB
14	21	M	1a, 1b	480	F1A1	34	32	NR	Training
15	27	M	1b	520	F1A1	62	39	NR	Training
16	31	F	2a	20	F1A1	63	36	SR	Training
17	35	M	2a	5.9	F1A1	72	34	SR	Training
18	37	F	1b	650	F1A1	219	58	NR	Training
19	37	M	1b	150	F0A1	79	74	TR	Training
20	37	M	2b	250	F1A1	225	29	TR	Training
21	40	M	2a	16	F1A2	211	129	SR	Training
22	42	M	1b	900	F3A2	86	139	TR	Training
23	49	M	1b	540	F1A1	100	30	TR	Training
24	51	F	1b	480	F1A1	80	34	NR	Training
25	52	M	1b	50	F1A2	96	79	SR	Training
26	53	M	1b	520	F4A2	97	90	NR	Training
27	57	M	1b	130	F1A2	61	37	TR	Training
28	57	M	2a	120	F1A2	164	53	SR	Training
29	59	F	1b	230	F3A2	70	38	NR	Training
30	59	M	2b	32	F1A1	162	119	NR	Training
31	62	F	1b	91	F1A2	90	34	NR	Training

ALT, alanine transaminase; γ-GT, γ-glutamyltransferase.

tumor necrosis factor-α.[7–9] In addition, we incorporated clinical information to help select genes; specifically, we included iron transporter–related genes, such as transferrin and the transferrin receptor, because iron depletion has been shown to enhance the efficacy of hepatitis C treatment.[19] Finally, we included some genes (eg, housekeeping genes) as controls for the microarray. Together, 295 genes were selected originally for the low-density cDNA microarray. Furthermore, after we developed the low-density cDNA microarray, interferon-stimulated genes were analyzed systematically by using a different microarray.[20] Another 452 genes that were derived mainly from interferon-, tumor necrosis factor–, and extracellular matrix–related genes were added to a new cDNA microarray that included a total of 747 genes.

Establishment of the Algorithm for Predicting Interferon Efficacy Based on Complementary DNA Microarray Data

As previously described,[15] we used a series of steps to make a reasonable prediction, including establishing a standard space database (SSDB), selecting characteristic parameters to differentiate groups of interest, setting variance–covariance, calculating the variance–covariance matrix, selecting a correlation/gene network, and, finally, calculating the Mahalanobis distance (MD) (the distance from the center of gravity can be determined for a new test sample using the SSDB), leading to a single parameter as a scale from multiple parameters. Thus, the SSDB dataset was selected from the SR patients that had clear clinical outcomes (13 members). This SSDB was trained by expanding it to different datasets, including SR/TR (10 members) and NR (8 members) data, to find genes that are expressed differentially between the 2 groups. The prediction probability of this stage was as follows: SR/TR (10 of 10; 100%), NR (7 of 8; 88%), with a P value of less than .0005.

By using the new prediction algorithm we assessed the accuracy of prediction using the 38 validation samples (31 SR/TR and 7 NR). We calculated the MD and scaled MD from this established dataset for each patient to determine the distance from the established SSDB center of gravity. At this point the calculation does not incor-

Table 2. Characteristics of the Core Patients Used for the SSDB and Training in Combination Therapy

Number	Age	Sex	Naive[a]	Serotype	Viral load (KIU/mL)	Histology/stage and activity	ALT (IU/L)	γ-GT (IU/L)	Clinical outcome	Use
1056	62	M	0	1	595	F4A3	199	87	SR	SSDB
1043	54	M	0	1	77	F2A2	95	80	SR	SSDB
1042	39	M	0	2	850	F1A1	59	89	SR	SSDB
1044	53	M	0	2	300	F3A1	194	147	SR	SSDB
1052	53	M	1	2	440	F1A1	97	80	SR	SSDB
1051	54	M	1	2	600	F3A1	30	22	SR	SSDB
1048	52	M	1	1	580	F1A0	81	37	SR	SSDB
1046	55	M	1	1	510	F1A2	68	49	SR	SSDB
1040	37	M	1	1	360	F1A1	45	90	SR	SSDB
1041	57	M	0	1	250	F4A2	159	93	SR	SSDB
1050	62	M	0	2	690	F1A2	118	96	SR	SSDB
1034	47	F	0	1	820	F1A1	39	43	TR	SSDB
1026	57	M	1	1	550	F3A2	106	14	TR	SSDB
1024	42	M	1	2	570	F2A2	639	83	TR	SSDB
1022	60	M	1	1	610	F1A1	56	209	TR	SSDB
1035	55	F	0	1	360	F1A2	131	42	TR	SSDB
1025	58	F	0	1	850	F1A1	58	35	TR	SSDB
1028	52	M	1	1	650	F1A1	44	17	TR	SSDB
1029	46	M	1	1	850	F1A1	40	30	TR	SSDB
1031	53	M	0	1	690	F2A2	83	52	TR	SSDB
1033	61	M	0	1	850	F2A2	64	46	TR	SSDB
1027	59	M	0	1	630	F3A2	79	59	TR	SSDB
1023	61	M	1	2	300	F3A3	67	61	TR	SSDB
1036	44	M	1	1	850	F1A1	75	54	TR	SSDB
1020	64	F	0	2	850	F1A2	358	76	TR	SSDB
1007	63	M	1	1	850	F3A2	257	132	NR	Training
1009	49	M	1	1	620	F3A1	346	274	NR	Training
1005	58	M	1	1	570	F3A1	87	42	NR	Training
1015	53	M	0	1	850	F1A1	37	65	NR	Training
1014	45	M	1	1	310	F2A2	125	187	NR	Training
1013	57	F	1	1	440	F3A2	57	35	NR	Training
1006	40	M	1	1	> 850	F3A1	244	237	NR	Training
1011	57	M	0	1	> 850	F2A2	90	48	NR	Training

ALT, alanine transaminase; γ-GT, γ-glutamyltransferase.
[a]0, first treatment; 1, retreatment.

porate any viral information such as genotype or viral load. The prediction probability of the validation stage was as follows: SR/TR (30 of 31; 97%) and NR (6 of 7; 86%). The *P* value, calculated using the χ^2 test, was less than .00001 for prediction accuracy. During the development of the algorithm we found several genes that were expressed differentially between the NR and SR/TR groups. The highlighted 75 genes according to *t*-test values are presented in Table 3. These could be separated into distinct groups such as interferon-, lipid metabolism–, complement-, and oxidoreductase-related genes. Because we used an artificial reference RNA as a control,[15] we were unable to determine whether the up- or down-regulation of these genes was meaningful biologically. *F*-test and *t*-test values for each gene, which represent the comparative expression levels between the SR/TR and NR groups, indicate only that the genes were expressed differentially between the SR/TR and NR groups.

Subsequently, we further analyzed samples from ribavirin combination therapy by using a DNA microarray containing 295 genes. The algorithm developed from the interferon monotherapy samples was ineffective for the samples from the combination therapy. Therefore, we tried to establish a new algorithm based on the data from this 295-gene DNA microarray but failed to obtain accurate prediction even using training samples from the combination therapy group (data not shown). To solve this problem we developed a new algorithm based on a new DNA microarray that included an additional 452 genes. The resulting algorithm allowed prediction of the outcome as follows: training (33 samples) stage: SR/TR (25 of 25; 100%) and NR (7 of 8; 88%); and validation (23 samples) stage: SR/TR (15 of 16; 94%) and NR (5 of 7; 71%), with prediction accuracies of 97% ($P < .0001$) and 87% ($P < .05$), respectively. Thus, the new microarray and algorithm could attain a high accuracy for prediction of treatment outcome using pretreatment liver

Table 3. Genes Differentially Expressed Between SR/TR and NR Groups in Monotherapy

GenBank number	Gene name	*F*-test	*t*-test
U05340	Cell division cycle 20 homolog (*S cerevisiae*)(CDC20)	.020	.169
BC008767	Acyl-coenzyme A oxidase 1, palmitoyl (ACOX1)	.123	.066
AF279437	Interleukin 22	.005	.201
M36807	Glycogen phosphorylase type IV	.007	.250
X03663	Colony-stimulating factor 1 receptor	.254	.096
X02750	Protein C (inactivator of coagulation factors Va and VIIIa)	.020	.172
BC000337	Glucose-6-phosphate dehydrogenase	.146	.066
BC009345	NADH dehydrogenase 1	.082	.233
X00566	Apolipoprotein A-1	.183	.063
BC001188	Transferrin receptor (p90, CD71)	.014	.395
J04026	Thioredoxin	.050	.160
S57235	CD68 antigen	.071	.377
M62403	Insulin-like growth factor binding protein 4	.010	.113
M65128	FK506-binding protein 2 (13 kD)	.050	.023
M29145	Hepatocyte growth factor	.115	.034
M11220	Granulocyte-macrophage colony stimulating factor	.000	.076
M55654	TATA box binding protein	.111	.036
X05360	Cell division cycle 2, G1 to S and G2 to M	.193	.043
M21097	CD19 antigen	.155	.059
J03171	Interferon (α, β, and ω receptor 1	.002	.032
U58196	Interleukin enhancer binding factor 1	.052	.032
Z12020	p53-associated gene; Mdm2, transformed 3T3 cell double minute 2	.014	.121
M93311	Metallothionein-III (growth inhibitory factor [neurotrophic])	.010	.062
X01992	Intereferon γ	.001	.156
Y14736	Immunoglobulin κ (light chain) variable 1D8	.030	.276
M22538	NADH dehydrogenase (ubiquinone) flavoprotein 2, 24 kilodaltons	.087	.172
X00955	Apolipoprotein A-II	.019	.292
U94586	NADH: ubiquinone oxidoreductase MLRQ subunit	.232	.046
X15949	Interferon-regulatory factor-2	.298	.093
M19154	Transforming growth factor β-2	.005	.078
X04688	Interleukin 5 (colony-stimulating factor, eosinophil)	.050	.173
M14505	Cyclin-dependent kinase 4	.116	.080

NOTE. Genes having *F*-test and *t*-test *P*-values <.4 and either value under .1 are listed.
Although *t*-test *P* values were calculated in Welch's method in cases in which the *F*-test *P* value <.05, the Student *t*-test method was applied in cases >.05.

samples. Interestingly, a different set of genes was highlighted in this study, including cyclophilin A and multidrug resistance protein 1 (Table 4).

Discussion

In the current study we developed an algorithm for predicting the efficacy of interferon treatment in hepatitis C patients based only on host microarray data. Once the microarray dataset was normalized, we searched for the most suitable statistical method to differentiate it. We chose a statistical method based on the MD[15] because it allows the maximal flexibility in data dispersion. By using this method we were able to obtain a distinct separation of the NR and the SR/TR groups. In our algorithm we used a gene network system rather than a set of independent differentially expressed genes to generate the categories. Thus, none of the genes listed in Table 3 with *t*-test and *F*-test values alone was able to provide any definitive information for classification, and none of the genes could predict the classification independently. Despite this, we were able to validate our new algorithm using a separate validation group. We were able to predict SR/TR patients accurately in 30 of 31 cases (97%) and NR patients in 6 of 7 cases (86%). The *P* value for these predictions was less than .00001, which is acceptable for prediction purposes and suggests that the dataset from the low-density cDNA microarray can predict NR and non-NR patients with high accuracy without any viral information. Pretreatment classification and identification of NR patients is useful because they have a higher risk than TR or SR patients for developing hepatocellular carcinoma.[3,4] This same approach also allowed prediction of the efficacy of interferon/ribavirin combination therapy with high accuracy. A different gene set was required for the establishment, however, which reflects the different underlying mechanism of the drug action between the 2 treatment regimens.

Genes were selected for the SSDB based on differential expression in our cDNA microarray. Besides interferon-

Table 4. Gene List Highlighted as Differentially Expressed in Combination Therapy

GenBank number	Gene name	*F*-test	*t*-test
X66362	PCTAIRE-3 for serine/threonine protein kinase	.007	.000
U90551	Histone (H2A II; histone 2A-like protein)	.054	.002
Y00285	Insulin-like growth factor II receptor	.027	.002
X03884	CD3 epsilon (T3 epsilon chain [20K] of T-cell receptor)	.045	.007
U12779	MAP kinase-activated protein kinase 2	.143	.008
Z33642	Leukocyte surface protein V7; immunoglobulin superfamily, member 2	.086	.010
U49837	LIM protein (cystein-rich protein 3)	.001	.011
M77349	BIGH3, TGF-β–induced product, TGF-β–induced 68 kilodalton	.141	.013
L16499	Orphan homeobox protein; hematopoietically expressed homeobox	.017	.013
X78817	ρ-GAP hematopoietic protein C1; ρ guanosine triphosphatase–activating protein 4	.070	.016
AF159442	Phospholipid scramblase 3	.000	.017
J04164	Interferon-inducible transmembrane protein 9–27	.199	.018
L41351	Serine protease 8 (prostatin)	.033	.019
U62437	Nicotinic acetylcholine receptor β2 subunit prexursor	.052	.020
X58072	GATA binding protein 3; transacting T-cell–specific transcription factor	.132	.027
X53414	L-alanine: glyoxylate transaminase	.021	.030
Y00052	Cyclophilin A (peptidylprolyl isomerase A; T-cell cyclophilin)	.152	.034
BC004490	Fos	.002	.035
U03397	Tumor necrosis factor–receptor superfamily, member 9	.140	.035
Z47087	Pol V elongation factor-like protein; S-phase kinase-associated protein 1A	.190	.047
M14758	Multiple drug resistance protein 1; P-glycoprotein	.066	.047
U61397	Ubiquitin-homology domain protein PIC1 (sentrin)	.021	.050
U16031	Interleukin-4–induced transcription factor, signal transducer and activator of transcription 6	.194	.050
BC032130	Asialoglycoprotein receptor 1	.032	.057
X05610	Type IV collagen alpha (2)	.046	.059
D23661	Ribosomal protein L37	.035	.066
X69150	Ribosomal protein S18	.013	.068
M15400	Retinoblastoma susceptibility	.040	.104
NM_001012	Ribosomal protein S8	.037	.133
M31627	X-box binding protein-1	.005	.198

NOTE. Both *F*-test and *t*-test values less than .2 are listed.

related genes, the SSDB includes genes related to immune response, stress, metal transport, and lipid metabolism. The inclusion of genes controlled by the interferon signal cascade and related to the immune response is not surprising. In addition, genes associated with lipid metabolism are not unexpected because HCV has a high affinity for lipids.[21,22] Furthermore, lipoprotein receptors were reported as HCV receptor candidates.[23,24] In fact, the involvement of lipid metabolism–related genes is described in depth in a study of HCV clearance in the chimpanzee by GeneChip analysis.[25] Therefore, the lipid metabolism–related genes that we included in our analysis could be targets for future study and therapeutic intervention. Finally, the presence of iron transport–related genes in the SSDB corresponds with the use of blood depletion therapies to reduce liver inflammation in hepatitis patients. It also may be of interest to study how genes in the SSDB, including additional metal-related genes such as metallothioneins, play a role in interferon efficacy.

These findings suggest that the TR patients have an anti-HCV interferon response similar to that of the SR patients. Indeed, it is possible that these TR patients may have become SR patients if interferon treatment was administered for more than 6 months because there is a significant effect of treatment duration in the efficacy of interferon treatment for chronic hepatitis C.[26] This observation is consistent with a study of chimpanzee HCV cases based on oligo-chip data.[25] Furthermore, the fact that we could predict the NR group without any viral information suggests that, in these cases, the host has an unfavorable response to the interferon treatment, which also suggests that, as in the SR group, there is an interaction between the host and the virus. Understanding the host response to interferon in NR patients could provide interesting targets for the development of new treatments for HCV.

In conclusion, we have established a low-density cDNA microarray for predicting interferon efficacy in chronic hepatitis C patients. Based only on host messenger RNA expression profiles from pretreatment biopsy samples, we can categorize patients successfully into SR/TR and NR groups with over 90% accuracy.

References

1. Yoshioka K, Kakumu S, Wakita T, et al. Detection of hepatitis C virus by polymerase chain reaction and response to interferon-